NASA TECHNICAL NOTE

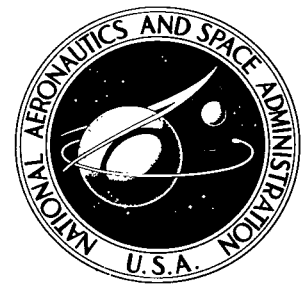

NASA TN D-6119

NASA TN D-6119

QUANTITATIVE DETERMINATION OF OPTICAL IMPERFECTIONS BY MATHEMATICAL ANALYSIS OF THE FOUCAULT KNIFE-EDGE TEST PATTERN

by Samuel Katzoff

Langley Research Center
Hampton, Va. 23365

NATIONAL AERONAUTICS AND SPACE ADMINISTRATION • WASHINGTON, D. C. • AUGUST 1971

1. Report No.	2. Government Accession No.	3. Recipient's Catalog No.
NASA TN D-6119		

4. Title and Subtitle	5. Report Date
QUANTITATIVE DETERMINATION OF OPTICAL IMPERFECTIONS BY MATHEMATICAL ANALYSIS OF THE FOUCAULT KNIFE-EDGE TEST PATTERN	August 1971
	6. Performing Organization Code

7. Author(s)	8. Performing Organization Report No.
S. Katzoff	L-7439
	10. Work Unit No.
9. Performing Organization Name and Address	188-78-51-05
NASA Langley Research Center Hampton, Va. 23365	11. Contract or Grant No.
	13. Type of Report and Period Covered
12. Sponsoring Agency Name and Address	Technical Note
National Aeronautics and Space Administration Washington, D.C. 20546	14. Sponsoring Agency Code

15. Supplementary Notes

16. Abstract

Linfoot developed an integral expression for the distribution of light intensity across the image of a lens or mirror when it is tested by the Foucault knife-edge method. This paper presents a fairly convenient method of inverting the linearized form of this expression so that the errors in the figure can be determined quantitatively from measurements of this light-intensity distribution. Essentially, the method consists of making a Fourier analysis of the deviation of the light intensity from that for a perfect lens or mirror and then summing the errors corresponding to the different terms of the Fourier series. The method is developed both for mirrors (or lenses) without central obscurations and for mirrors with central obscurations (Cassegrain type). Calculated examples of several cases for both types are included.

17. Key Words (Suggested by Author(s))	18. Distribution Statement
Foucault knife-edge test Integral equations Large orbiting telescope Active optics Deformable mirror	Unclassified – Unlimited

19. Security Classif. (of this report)	20. Security Classif. (of this page)	21. No. of Pages	22. Price*
Unclassified	Unclassified	50	$3.00

*For sale by the National Technical Information Service, Springfield, Virginia 22151

QUANTITATIVE DETERMINATION OF OPTICAL IMPERFECTIONS BY MATHEMATICAL ANALYSIS OF THE FOUCAULT KNIFE-EDGE TEST PATTERN

By S. Katzoff
Langley Research Center

SUMMARY

Linfoot developed an integral expression for the distribution of light intensity across the image of a lens or mirror when it is tested by the Foucault knife-edge method. This paper presents a fairly convenient method of inverting the linearized form of this expression so that the errors in the figure can be determined quantitatively from measurements of this light-intensity distribution. Essentially, the method consists of making a Fourier analysis of the deviation of the light-intensity distribution from that for a perfect lens or mirror, and then summing the errors that correspond to the different terms of the Fourier series. The method is developed both for mirrors (or lenses) without central obscurations and for mirrors with central obscurations (Cassegrain type).

Various examples are worked out for both types, both to show the practicability of the method and to show the relationships between the error in the figure and the deviations of the knife-edge test pattern from the normal.

Some discussion has been included concerning application of the method to the testing of a large orbiting telescope, possible limitations to the basic theory of the knife-edge test, and the desirability of solving the same problem for the case when the errors are so large that the present linearized theory is either inexact or totally inapplicable.

INTRODUCTION

A number of laboratories, including the NASA Langley Research Center, have been actively involved in studying the problems associated with a large orbiting telescope. In order that the telescope might take full advantage of the perfect seeing that exists outside the atmosphere, it should have an essentially diffraction-limited performance. Accordingly, an appreciable part of this study effort has been devoted to problems associated with achieving and maintaining such perfection. To manufacture the primary mirror for such a telescope, while accurately allowing for (or compensating for) gravity, is itself a

formidable task. Then, even if the telescope is diffraction-limited when it goes into orbit, temperature nonuniformity and possibly material relaxation or creep may subsequently introduce distortions.

On the basis of such considerations, it is apparent that some method of in-orbit testing is desirable. If the primary mirror is made adjustable – for example, slightly flexible, with a system of jacks, or actuators, for adjusting the figure (see ref. 1) – it would be especially desirable that the test method be capable of providing quantitative information on the distortion that the adjustment mechanism must correct.

The Foucault knife-edge method offers a possible approach to solving the problem of in-orbit testing. It is widely used in the testing of lenses and mirrors because of its simplicity, sensitivity, and minimal equipment requirements. The method would seem to be especially suited to testing the optics of a large telescope in orbit because the essential requirement of a perfectly uniform and perfectly collimated test beam of adequate intensity is satisfied in outer space by the light from any sufficiently bright star. The usual cut-and-try method of removing any revealed imperfections, however, hardly seems to be applicable to a mirror in orbit, although it is possibly not completely impractical. In any case, a quantitative analytical approach to interpreting the knife-edge-test observations seems better adapted to automation of the test and correction procedure.

This problem – the quantitative interpretation of the appearance of the mirror under the knife-edge test – is the subject of the present paper. The approach starts from the analysis of Linfoot (ref. 2) who derived expressions for the distribution of light intensity in the knife-edge test pattern for the perfect mirror, and also for the imperfect mirror as a function of the surface distortion (more specifically, as a function of the intensity and phase distortion of the converging spherical wave front as it leaves the mirror). For a uniformly reflecting mirror with relatively slight inaccuracies in the figure, the corresponding change in the pattern from that for a perfect mirror is given by a linear integral expression involving the phase distortion of the converging wave front at the mirror. Solving for this phase distortion (in effect, solving for the distortion of the mirror surface) amounts to inverting this integral expression.

Thus, the problem of quantitatively interpreting the knife-edge observations reduces to the problem of solving an integral equation. A method of solving the equation is presented herein. In the meantime, Dr. B. E. Gatewood at Ohio State University has studied various other approaches under an NASA grant (ref. 3).

The present paper reviews the method of solving the integral equation for two basic cases, namely (1) the mirror without a central obscuration, which will be referred to as a simple mirror, and (2) the mirror with a central obscuration, as in a Cassegrain arrangement. Several examples are analyzed, including the examples analyzed in

reference 3. Because high accuracy requires large computational effort, the accuracy in these examples (determined by the number of terms in the Fourier series that represents the solution) was limited to that sufficient to show the main characteristics of the methods.

A few remarks have been included concerning the actual procedure of applying the knife-edge method to study the distortion over the entire surface of a mirror. These remarks are of a general nature and do not go into the important mechanical and instrumentation problems that would have to be solved in order to make the knife-edge method practical for use with an orbiting telescope.

SYMBOLS

$D(x,y)$ electric wave displacement at the (x,y) image point in the observation plane; normalized so that it would equal $E(x,y)$ for perfect optics and with knife-edge removed

$E(x,y)$ electric wave displacement at (x,y) on the converging wave front just as it leaves the mirror; amplitude normalized to unity

$I(x)$ intensity (see eq. (3))

$I_o(x)$ intensity for a perfect mirror

$[M], [F], [C]$ matrices defined in the text

$m(x)$ local depression of mirror surface below that for a perfect mirror, in half-wavelengths

$\{m\}$ vector whose elements are the values of m along a chord

P_n Legendre polynomial

$p(x)$ deviation of observed intensity from that for a perfect mirror (see eq. (4))

$\{p\}$ vector whose elements are the values of p along a chord

R one-half the width of gap in chord, for mirror with a central obscuration (For all calculated examples, $R = 5/41$, relative to chord or diameter equal to 2.)

t	dummy variable corresponding to x
X,Y	coordinate axes
x	distance normal to knife-edge, normalized such that length of chord being studied is 2
y	distance parallel to knife-edge
z	distance used in defining bump on mirror surface for two examples from reference 3; 5x - 3
θ	dummy variable corresponding to ϕ

$\phi = \cos^{-1}x$

Subscripts:

a	antisymmetrical
l	left side of chord (negative x)
r	right side of chord (positive x)
s	symmetrical

OPTICAL ARRANGEMENT

A schematic sketch of the arrangement of the optical elements is shown in sketch (a). The knife edge passes precisely through the focus of the mirror, and the lens, which is located directly behind the knife edge, focuses the mirror surface onto the indicated mirror image plane. This image plane might contain, for example, a raster of photosensitive sensors, a single line of such sensors, or possibly a single sensor mounted so that it can scan a line across the image. With the knife edge normal to the plane of the sketch, as shown, the scan line would be in, or parallel to, the plane of the sketch.

Sketch (a) shows a perfectly collimated beam (as of starlight) and a parabolic mirror. In a typical laboratory test, with a spherical mirror, both the light source and the knife-edge are close to the center of curvature. Although such an arrangement is geometrically different from that of figure 1, both arrangements serve to produce a converging

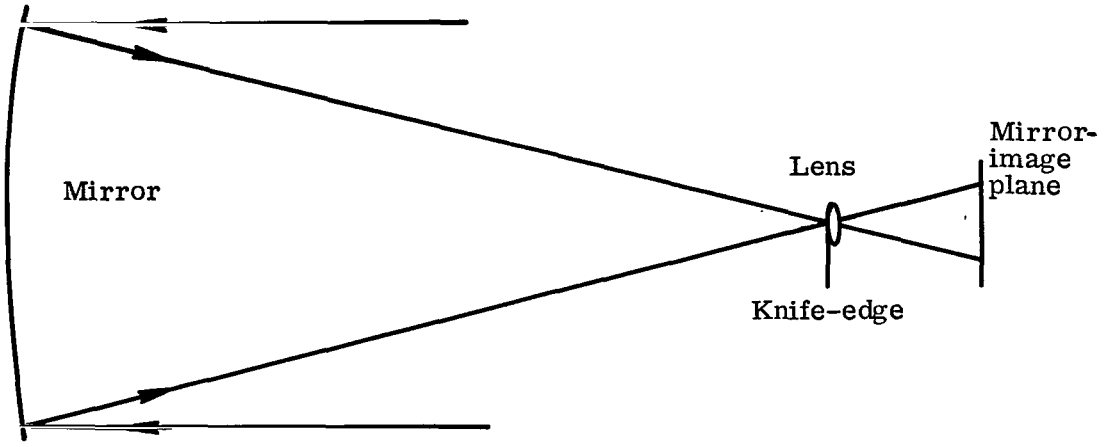

Sketch (a)

spherical wave front which comes to a focus at the knife-edge; and the analyses of reference 2 and of the present paper apply equally well to both cases.

With regard to accurate placement of the knife-edge, the focus of the mirror is not strictly definable if the mirror is imperfect. A related fact is that, even if the mirror is perfect, mislocating the knife-edge will produce a pattern in the focal plane of the lens which indicates that the mirror is canted, has spherical aberration, or both (ref. 2). With a flexible mirror one could, presumably, then distort and rotate the mirror until it appears as a perfect mirror with its focus precisely on the mislocated knife-edge. However, it would be more reasonable to try to minimize the forces exerted by the actuators on the mirror – that is, to set the knife-edge carefully at approximately the "best focus," as indicated by the general appearance of the pattern, before proceeding to analyze the pattern and then correct the residual distortions with the actuators. Such an approach is also desirable with regard to quantitative analysis of the pattern, because accurate analysis by the present linearized method does, in fact, require that the distortions be small – say, of the order of one-tenth of a wavelength or less.

EQUATION FOR THE SIMPLE MIRROR

Derivation of Linearized Equation

General equation.- Let $E(x,y)$ be the electric wave displacement at point (x,y) in the mirror surface. Let $D(x,y)$ be the electric wave displacement at the corresponding image point in the observation plane (mirror-image plane, sketch (a)). In order to simplify the form of the equation, the measure of $D(x,y)$ is adjusted so that if the knife-edge were absent along with the corresponding diffraction phenomena, $D(x,y)$ would be the

same as $E(x,y)$ for a perfect mirror. Then, with the knife-edge passing through the nominal focal point of the mirror, the relation between $D(x,y)$ and $E(x,y)$, as given by Linfoot, is

$$2\pi D(x,y) = \pi E(x,y) + i \int_{-1}^{1} \frac{E(t,y)}{t - x}\, dt \qquad (1)$$

where

x	distance normal to knife-edge
y	distance parallel to knife-edge
t	dummy variable corresponding to x

Sketch (b) will help to clarify this equation. The circle represents the mirror (or its image produced by the small lens), and the knife-edge is parallel to the Y-axis. The form of the equation shows that

(1) Along any chord normal to the knife edge (that is, for a fixed y), D is determined only by E along the same chord, and thus is not affected by any other part of the mirror surface. This independence of each chord is a valuable simplification in analyzing the knife-edge pattern. The parameter y will be omitted from subsequent equations, since it will be understood that the analysis is always concerned with some particular chord.

(2) Since the factor $dt/(t - x)$ in the integral is nondimensional, any convenient unit may be used for the linear dimensions. Any chord that is under consideration may thus be considered to extend from $x = -1$ to $x = +1$, as indicated in sketch (b) and in the limits of the integral.

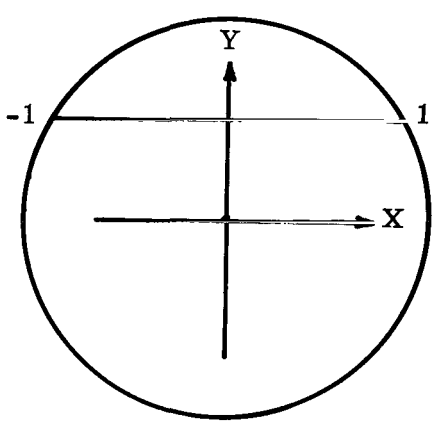

Sketch (b)

Linearized equation.- Let $E(x) = 1$ for a perfect mirror. Then, if, at points x, the mirror surface is depressed by $m(x)$ half-wavelengths, $E(x)$ will be given by

$$E(x) = e^{-2\pi i m(x)} = 1 - 2\pi i m(x) - 2\pi^2 m^2(x) + \ldots$$

When this approximation is introduced into equation (1), the equation becomes

$$2\pi D(x) = \pi\left[1 - 2\pi^2 m^2(x) + 2\int_{-1}^{1} \frac{m(t)}{t - x}\,dt\right] + i\left[-2\pi^2 m(x) + \int_{-1}^{1} \frac{dt}{t - x} - 2\pi^2 \int_{-1}^{1} \frac{m^2(t)}{t - x}\,dt\right] \tag{2}$$

Multiplying both sides of the equation by their complex conjugates, and retaining only the first-order terms in m gives the following equation for the intensity:

$$I(x) = 4\pi^2 \left|D(x)\right|^2 = \pi^2 + \ln^2\left(\frac{1 - x}{1 + x}\right) + 4\pi^2 \int_{-1}^{1} \frac{m(t)\,dt}{t - x} - 4\pi^2 m(x) \ln \frac{1 - x}{1 + x} \tag{3}$$

The sum of the first two terms on the right side, $\pi^2 + \ln^2(1 - x)/(1 + x)$, is the intensity $I_0(x)$ for a perfect mirror. It is plotted in figure 1. The remaining two terms give the difference between the intensity for the imperfect mirror and that for a perfect mirror. Equation (3) is accordingly rearranged and rewritten as follows:

$$\frac{I(x) - I_0(x)}{4\pi^2} \equiv p(x) = \int_{-1}^{1} \frac{m(t)}{t - x}\,dt - m(x) \ln \frac{1 - x}{1 + x} \tag{4}$$

The solution of this equation, where $p(x)$ is given and $m(x)$ is to be determined, is the present problem.

Examples of $p(x)$ Corresponding to Some Simple $m(x)$ Distributions

Substituting some simple algebraic expressions for m in the preceding equation will help to show some general characteristics of the relation between $m(x)$ and $p(x)$. First, since $m(x) \ln (1 - x)/(1 + x)$ is the same as $\int_{-1}^{1} m(x)\,dt/(t - x)$, equation (4) is rewritten as

$$p(x) = \int_{-1}^{1} \frac{m(t) - m(x)}{t - x}\,dt \tag{5}$$

Example A-1.- If m is a constant, $m(t) - m(x)$ is zero and hence $p(x)$ is zero. In other words, a uniform phase change across the entire wave front has no discernible effect on the image behind the knife-edge (which fact is physically apparent, and also mathematically apparent since, in the derivation of the original equation, the reference phase was arbitrary). An alternative interpretation is that replacing the parabolic mirror with a smaller or larger, geometrically similar, mirror with the same focal point leaves the pattern unchanged when the mirror is tested with a perfectly collimated beam as in sketch (a). This ambiguity is not altogether trivial, as will appear in a later section in which analysis of the entire mirror image is discussed.

Example A-2.- Let $m(x) = ax$; that is, let m vary linearly along the chord. Then

$$p(x) = a \int_{-1}^{1} \frac{t - x}{t - x}\, dt = 2a$$

Thus, for the case of a linearly varying m, $p(x)$ is a constant. As was pointed out in reference 2, this case could correspond to a slight rotation of the entire mirror about a line through its center parallel to the knife-edge, or to a slight shift of the knife-edge, in the mirror focal plane, so that it no longer passes exactly through the focal point.

Example A-3.- Let $m(x) = ax^2$. Then

$$p(x) = a \int_{-1}^{1} \frac{t^2 - x^2}{t - x}\, dt = 2ax$$

Other cases in which $m(x)$ is simply an integral power of x are similarly easily calculated. Table I gives the first few of these and also gives the general formula. It will be seen from table I that if m is an even function of x, p is an odd function of x, and if m is an odd function of x, p is an even function of x.

Table I may be inverted to derive table II, which shows $m(x)$ corresponding to $p(x) = x^n$. The coefficients in the expressions for $m(x)$ are easily obtained by a recursive procedure, which will be given later. (See bottom of p. 12.)

Inversion in Power Series or in Series of Polynomials

A possible method of solving equation (4) or equation (5) is immediately apparent: Analyze the experimental $p(x)$ distribution into a power series in x,

$$p(x) = a + bx + cx^2 + dx^3 + \ldots$$

and the mirror distortion will be given directly by the sum of the corresponding m terms from table II

$$m(x) = \frac{a}{2}x + \frac{b}{2}x^2 + \frac{c}{2}\left(x^3 - \frac{x}{3}\right) + \frac{d}{2}\left(x^4 - \frac{x^2}{3}\right) + \ldots$$

TABLE I.- p(x) FOR $m(x) = x^n$; SIMPLE MIRROR

m(x)	p(x)
1	0
x	2
x^2	2x
x^3	$2\left(x^2 + \frac{1}{3}\right)$
x^4	$2\left(x^3 + \frac{x}{3}\right)$
x^5	$2\left(x^4 + \frac{x^2}{3} + \frac{1}{5}\right)$
x^6	$2\left(x^5 + \frac{x^3}{3} + \frac{x}{5}\right)$
.	.
.	.
.	.
x^n	$2\left(x^{n-1} + \frac{x^{n-3}}{3} + \frac{x^{n-5}}{5} + \ldots + \frac{1}{n}\right)$ (n odd) $2\left(x^{n-1} + \frac{x^{n-3}}{3} + \frac{x^{n-5}}{5} + \ldots + \frac{x}{n-1}\right)$ (n even)

TABLE II.- m(x) FOR $p(x) = x^n$; SIMPLE MIRROR

p(x)	m(x)
1	$\frac{1}{2}x$
x	$\frac{1}{2}x^2$
x^2	$\frac{1}{2}\left(x^3 - \frac{x}{3}\right)$
x^3	$\frac{1}{2}\left(x^4 - \frac{x^2}{3}\right)$
x^4	$\frac{1}{2}\left(x^5 - \frac{x^3}{3} - \frac{4x}{45}\right)$
x^5	$\frac{1}{2}\left(x^6 - \frac{x^4}{3} - \frac{4x^2}{45}\right)$
x^6	$\frac{1}{2}\left(x^7 - \frac{x^5}{3} - \frac{4x^3}{45} - \frac{44x}{945}\right)$
.	.
.	.
.	.

A modification of this approach would be to analyze the experimental p(x) distribution into a sum of orthogonal polynomials, say the Legendre polynomials P_n, and again sum the corresponding m terms. For this approach, one would need a table like table III, in which the p terms of table II have been combined to form the Legendre polynomials, and in which the corresponding m terms of table II have been combined.

TABLE III.- m(x) FOR $p(x) = P_n(x)$; SIMPLE MIRROR

p(x)	m(x)
$P_0 \equiv 1$	$\frac{x}{2}$
$P_1 \equiv x$	$\frac{x^2}{2}$
$P_2 \equiv \frac{1}{2}\left(3x^2 - 1\right)$	$\frac{1}{2}\left(\frac{3}{2}x^3 - x\right)$
$P_3 \equiv \frac{1}{2}\left(5x^3 - 3x\right)$	$\frac{1}{2}\left(\frac{5}{2}x^4 - \frac{7}{3}x^2\right)$
$P_4 \equiv \frac{1}{8}\left(35x^4 - 30x^2 + 3\right)$	$\frac{1}{2}\left(\frac{35}{8}x^5 - \frac{125}{24}x^3 + \frac{89}{72}x\right)$
.	.
.	.
.	.

A considerable amount of algebra would be involved in setting up such a table if a large number of Legendre polynomials is used in order to attain an acceptable accuracy, although the effort would hardly be prohibitive. In any case, it was finally decided that a similar Fourier-series approach would be somewhat more practical and generally more attractive. The following section describes the Fourier-series method, which is presented as the preferred method. The material of the preceding tables will accordingly not be further used; it was presented because it showed most directly the relations between p(x) and m(x) and the nature of the proposed approach to solving the integral equation.

SOLUTION IN FOURIER SERIES; SIMPLE MIRROR

Correspondence Between p and m Expressed in Terms of $\cos^n\phi$

In equation (5)

$$p(x) = \int_{-1}^{1} \frac{m(t) - m(x)}{t - x}\, dt$$

substitute $x = \cos \phi$, $t = \cos \theta$, where θ is now the dummy variable corresponding to ϕ. The equation now takes the form

$$p(\phi) = \int_0^{\pi} \frac{m(\theta) - m(\phi)}{\cos \theta - \cos \phi} \sin \theta \, d\theta \tag{6}$$

Putting $m(\phi) = 1$, $\cos \phi$, $\cos^2\phi$, $\cos^3\phi$, and so forth simply reproduces table I, x being replaced by $\cos \phi$. Inverting simply reproduces table II, similarly altered. These revised tables are shown here as tables IV and V.

TABLE IV.- $p(\phi)$ FOR $m(\phi) = \cos^n\phi$; SIMPLE MIRROR

$m(\phi)$	$p(\phi)$
1	0
$\cos \phi$	2
$\cos^2\phi$	$2 \cos \phi$
$\cos^3\phi$	$2\left(\cos^2\phi + \frac{1}{3}\right)$
.	.
.	.
.	.

TABLE V.- $m(\phi)$ FOR $p(\phi) = \cos^n\phi$; SIMPLE MIRROR

$p(\phi)$	$m(\phi)$
1	$\frac{1}{2} \cos \phi$
$\cos \phi$	$\frac{1}{2} \cos^2\phi$
$\cos^2\phi$	$\frac{1}{2}\left(\cos^3\phi - \frac{\cos \phi}{3}\right)$
$\cos^3\phi$	$\frac{1}{2}\left(\cos^4\phi - \frac{\cos^2\phi}{3}\right)$
.	.
.	.
.	.

Correspondence Between p and m Expressed in Terms of $\cos n\phi$

One may now group the p terms of table V to form $\cos \phi$, $\cos 2\phi$, . . ., by using the formulas (ref. 4, item 3.175)

$$\left.\begin{aligned}
\cos 2\phi &= 2\cos^2\phi - 1 \\
\cos 3\phi &= 4\cos^3\phi - 3\cos\phi \\
\cos 4\phi &= 8\cos^4\phi - 8\cos^2\phi + 1 \\
\cos 5\phi &= 16\cos^5\phi - 20\cos^3\phi + 5\cos\phi \\
&\;\;\vdots \qquad\qquad \vdots \\
\cos n\phi &= 2^{n-1}\cos^n\phi - \frac{n}{1!}\,2^{n-3}\cos^{n-2}\phi \\
&\quad + \frac{n(n-3)}{2!}\,2^{n-5}\cos^{n-4}\phi - \frac{n(n-4)(n-5)}{3!}\,2^{n-7}\cos^{n-6}\phi \\
&\quad + \frac{n(n-5)(n-6)(n-7)}{4!}\,2^{n-9}\cos^{n-8}\phi - \ldots
\end{aligned}\right\} \qquad (7)$$

Grouping the corresponding powers of $\cos \phi$ in the m terms yields, finally, the corresponding pairs of p and m shown in table VI. The coefficients in the expressions for the m terms in this table are related as follows:

$$-\frac{1}{3} = -\frac{1}{3}$$

$$-\frac{4}{45} = -\frac{1}{5} + \frac{1}{3}\times\frac{1}{3}$$

$$-\frac{44}{945} = -\frac{1}{7} + \frac{1}{5}\times\frac{1}{3} + \frac{1}{3}\times\frac{4}{45}$$

$$-\frac{428}{14\ 175} = -\frac{1}{9} + \frac{1}{7}\times\frac{1}{3} + \frac{1}{5}\times\frac{4}{45} + \frac{1}{3}\times\frac{44}{945}$$

$$-\frac{10\ 196}{467\ 775} = -\frac{1}{11} + \frac{1}{9}\times\frac{1}{3} + \frac{1}{7}\times\frac{4}{45} + \frac{1}{5}\times\frac{44}{945} + \frac{1}{3}\times\frac{428}{14\ 175}$$

TABLE VI.- $m(\phi)$ FOR $p(\phi) = \cos n\phi$; SIMPLE MIRROR

$p(\phi)$	$m(\phi)$ (*)
1	$\frac{1}{2}\cos\phi$
$\cos\phi$	$\frac{1}{4}\cos 2\phi$
$\cos 2\phi$	$\frac{1}{4}\left(\cos 3\phi - \frac{1}{3}\cos\phi\right)$
$\cos 3\phi$	$\frac{1}{4}\left(\cos 4\phi - \frac{1}{3}\cos 2\phi\right)$
$\cos 4\phi$	$\frac{1}{4}\left(\cos 5\phi - \frac{1}{3}\cos 3\phi - \frac{4}{45}\cos\phi\right)$
$\cos 5\phi$	$\frac{1}{4}\left(\cos 6\phi - \frac{1}{3}\cos 4\phi - \frac{4}{45}\cos 2\phi\right)$
$\cos 6\phi$	$\frac{1}{4}\left(\cos 7\phi - \frac{1}{3}\cos 5\phi - \frac{4}{45}\cos 3\phi - \frac{44}{945}\cos\phi\right)$
$\cos 7\phi$	$\frac{1}{4}\left(\cos 8\phi - \frac{1}{3}\cos 6\phi - \frac{4}{45}\cos 4\phi - \frac{44}{945}\cos 2\phi\right)$
$\cos 8\phi$	$\frac{1}{4}\left(\cos 9\phi - \frac{1}{3}\cos 7\phi - \frac{4}{45}\cos 5\phi - \frac{44}{945}\cos 3\phi - \frac{428}{14\,175}\cos\phi\right)$
$\cos 9\phi$	$\frac{1}{4}\left(\cos 10\phi - \frac{1}{3}\cos 8\phi - \frac{4}{45}\cos 6\phi - \frac{44}{945}\cos 4\phi - \frac{428}{14\,175}\cos 2\phi\right)$
$\cos 10\phi$	$\frac{1}{4}\left(\cos 11\phi - \frac{1}{3}\cos 9\phi - \frac{4}{45}\cos 7\phi - \frac{44}{945}\cos 5\phi - \frac{428}{14\,175}\cos 3\phi - \frac{10\,196}{467\,775}\cos\phi\right)$
$\cos 11\phi$	$\frac{1}{4}\left(\cos 12\phi - \frac{1}{3}\cos 10\phi - \frac{4}{45}\cos 8\phi - \frac{44}{945}\cos 6\phi - \frac{428}{14\,175}\cos 4\phi - \frac{10\,196}{467\,775}\cos 2\phi\right)$

*See the recursion procedure for deriving the coefficients in the expressions for the m terms.

Inversion Matrix

The method of solving for m, given p, is first to make a Fourier analysis of $p(\phi)$, and then to apply the coefficients to the corresponding m terms of table VI and add the results. Thus, if the Fourier analysis of $p(\phi)$ gives

$$p(\phi) = a_0 + a_1 \cos\phi + a_2 \cos 2\phi + a_3 \cos 3\phi + \ldots$$

the corresponding $m(\phi)$ is given by

$$m(\phi) = \frac{a_0}{2}\cos\phi + \frac{a_1}{4}\cos 2\phi + \frac{a_2}{4}\left(\cos 3\phi - \frac{1}{3}\cos\phi\right)$$

$$+ \frac{a_3}{4}\left(\cos 4\phi - \frac{1}{3}\cos 2\phi\right) + \ldots$$

(It will be noted that since $p(\phi)$ is defined only between 0 and π, it can be represented by a Fourier series containing only cosine terms.) In the example problems to be presented herein, 12-term series were used, for which both the programing and computing efforts were small in terms of modern computer technology and capability.

The computational procedure is essentially as follows:

(1) Locate 12 points along the mirror diameter or chord at $x = \cos 7.5^\circ$, $x = \cos 22.5^\circ$, $x = \cos 37.5^\circ$, . . ., $x = \cos 172.5^\circ$. The values of p at these points $\left(p_{7.5}, p_{22.5}, \cdots, p_{172.5}\right)$ arranged in a column form the vector $\{p\}$.

(2) Prepare a 12×12 Fourier matrix $[F]$ as shown

$$[F] \equiv \begin{bmatrix} \frac{1}{12} & \frac{1}{12} & \cdots & \frac{1}{12} \\ \frac{\cos 7.5^\circ}{6} & \frac{\cos 22.5^\circ}{6} & \cdots & \frac{\cos 172.5^\circ}{6} \\ \frac{\cos 15^\circ}{6} & \frac{\cos 45^\circ}{6} & \cdots & \frac{\cos 345^\circ}{6} \\ \frac{\cos 22.5^\circ}{6} & \frac{\cos 67.5^\circ}{6} & \cdots & \frac{\cos 517.5^\circ}{6} \\ \vdots & \vdots & \vdots & \vdots \\ \frac{\cos 82.5^\circ}{6} & \frac{\cos 247.5^\circ}{6} & \cdots & \frac{\cos 1897.5^\circ}{6} \end{bmatrix}$$

The product $[F]\{p\}$ is a vector containing the 12 coefficients $a_0, a_1, a_2, \ldots, a_{11}$ of the Fourier series. As will be seen, this step is not actually done.

Determining the Fourier coefficients in this manner amounts to using the trapezoid rule to evaluate

$$a_n = \frac{2}{\pi} \int_0^{\pi} p(\phi) \cos n\phi \, d\phi$$

One might suppose that a more sophisticated numerical-integration formula such as Simpson's one-third rule would give a more accurate result. Actually, however, in the case of a periodic function, there is no general justification for weighting any ordinate more than any other ordinate. Furthermore, where a finite number of Fourier terms must represent a curve passing through the same number of equally spaced points (as in the present problem), determining the coefficients by the trapezoid rule results in a curve that passes exactly through the given points. A proof of this interesting fact may be found in reference 5, section 4.

(3) Set up the 12×12 matrix $[M]$, whose elements are the 12 expressions for m in table VI evaluated for the 12 values of ϕ. Thus, the elements of the first column are $\frac{1}{2} \cos \phi$ evaluated for $\phi = 7.5^\circ, 22.5^\circ, \ldots, 172.5^\circ$; the elements of the second column are $\frac{1}{4} \cos 2\phi$ evaluated for these same values of ϕ; and so forth.

$$[M] \equiv \begin{bmatrix} \frac{\cos 7.5^\circ}{2} & \frac{\cos 15^\circ}{4} & \frac{\cos 22.5^\circ - \frac{1}{3}\cos 7.5^\circ}{4} & \cdots \\ \frac{\cos 22.5^\circ}{2} & \frac{\cos 45^\circ}{4} & \frac{\cos 67.5^\circ - \frac{1}{3}\cos 22.5^\circ}{4} & \cdots \\ \vdots & \vdots & \vdots & \vdots \\ \frac{\cos 172.5^\circ}{2} & \frac{\cos 345^\circ}{4} & \frac{\cos 517.5^\circ - \frac{1}{3}\cos 172.5^\circ}{4} & \cdots \end{bmatrix}$$

(4) Multiplying the vector of Fourier coefficients by the matrix $[M]$ finally gives a vector $\{m\}$ containing the values of m at the 12 points $x = \cos 7.5^\circ$, $x = \cos 22.5^\circ$, . . ., $x = \cos 172.5^\circ$.

Combining all these steps into one equation gives

$$\{m\} = [M][F]\{p\}$$

The 12×12 matrix $[M][F]$ is thus the basic result. Multiplying any experimental p vector $\{p\}$ by $[M][F]$ gives the corresponding m vector $\{m\}$ which represents the mirror distortion at the 12 points. This inversion matrix $[M][F]$ is given completely in the appendix. The number of significant figures shown is no doubt excessive; no effort was made to determine the optimum number of significant figures.

Example Problems

Three example problems were calculated by use of this inversion matrix. The first two were very simple ones that served mainly to verify that the basic concept of the method is correct and that there were no errors in the matrix. The third problem was the same one that was studied in reference 3. It corresponds to a narrow bump on the mirror, centered at $x = 0.6$, and of total width equal to 0.4. These three problems are reviewed in this section.

Problem A-1.- In the first problem, all the elements of the vector $\{p\}$ were unity $(1,1,1,\ldots,1)$. As seen in table III or table V, the corresponding m is simply $\frac{1}{2}x$ or $\frac{1}{2}\cos\phi$. The elements of the vector $\{m\}$ were indeed exactly $\frac{1}{2}\cos 7.5^\circ$, $\frac{1}{2}\cos 22.5^\circ$, $\frac{1}{2}\cos 37.5^\circ$, . . ., $\frac{1}{2}\cos 172.5^\circ$. The p and m curves are shown in figure 2(a).

Problem A-2.- In the second problem, p was taken as x^2 or $\cos^2\phi$ $\left(\text{which is equal to } \frac{1}{2} + \frac{1}{2}\cos 2\phi\right)$. As seen in table II or table V, the corresponding m is $\frac{1}{2}\left(x^3 - \frac{x}{3}\right)$ or $\frac{1}{2}\left(\cos^3\phi - \frac{1}{3}\cos\phi\right)$. The calculations produced this result exactly. The p and m curves are shown in figure 2(b).

The accuracies of the preceding two results simply exemplify that if p is exactly expressible in the form $a_0 + a_1\cos\phi + a_2\cos 2\phi + \ldots + a_{11}\cos 11\phi$, this procedure will give the corresponding values of m at the 12 points exactly. If, however, p cannot be satisfactorily represented with this 12-term series, the 12×12 inversion matrix will give a set of 12 m values that are correspondingly inexact.

Problem A-3.- The bump used for the third problem is shown in figure 3. It is best described in terms of a new variable z which has its origin at the center of the bump ($x = 0.6$) and a unit that is one-fifth the unit of x. Thus, $z = \frac{x - 0.6}{0.2} = 5x - 3$. The surface distortion is then given by

$$m(z) = 0 \qquad (z^2 \geqq 1)$$

$$m(z) = -(1 - z^2)^2 \qquad (z^2 \leqq 1)$$

The minus sign is used in front of the parenthesis because, in the derivation of equation (4), positive m was assumed to represent a depression.

In the analytical evaluation of p for this case, some caution must be exercised in using equation (4) or equation (5), because the analytical expression for the bump does not apply outside the bump. Nevertheless, the calculation is straightforward and is not detailed here. The result is

$$p = -2z^3 + \frac{10}{3} z - (1 - z^2)^2 \ln \left| \frac{1 - z}{1 + z} \frac{1 + x}{1 - x} \right| \qquad (z^2 \leq 1)$$

$$p = -2z^3 + \frac{10}{3} z - (1 - z^2)^2 \ln \left| \frac{1 - z}{1 + z} \right| \qquad (z^2 \geq 1)$$

This p distribution is shown in figure 3.

As before, the first step is to find the values of p at the 12 points $x = \cos 7.5^\circ$, $x = \cos 22.5^\circ$, . . ., $x = \cos 172.5^\circ$. With these values as the elements of the vector $\{p\}$, one can then determine the 12 elements of the vector $\{m\} = [M][F]\{p\}$. The 12 m values so obtained are plotted in figure 4. A curve faired through these points would show the bump, but not very accurately; in particular, the bump would be too low, although it would be in about the right location. The poor accuracy reflects the fact that only three points fall in the region of the main irregularity of the p curve, which are inadequate to define the p curve in the region (the region of the bump). It is apparent that if the mirror distortions can be as sharp as this bump, more than 12 points would have to be used (with correspondingly larger $[M]$, $[F]$, and $[M][F]$ matrices) if satisfactory accuracy is to be achieved. In the methods that were studied in reference 2, 40 points were used, with excellent results.

Although this bump probably represents an unrealistically sharp and narrow irregularity, it was decided to pursue the matter further by doubling the number of points. A 24×24 $[M][F]$ matrix was derived by extending the procedure used for deriving the 12×12 matrix; and a $\{p\}$ vector was determined by finding the values of p at $x = \cos 3.75^\circ$, $x = \cos 11.25^\circ$, $x = \cos 18.75^\circ$, . . ., $x = \cos 176.25^\circ$. The resulting m values, shown in the lower part of figure 4, are in very good agreement with the true m curve. The 24×24 $[M][F]$ matrix is presented in the appendix.

The fact that the entire computed m curve falls below the original m curve reflects the fact that the average value of a sum of $\cos n\phi$ terms (averaged with respect to ϕ, in the range between 0 and π) is zero. As explained previously, such a downward shift of the entire m curve by a constant is of no physical significance.

EQUATION FOR MIRROR WITH CENTRAL OBSCURATION

Derivation of Linearized Equation

For a mirror with a central obscuration (Cassegrain type), one may again, for simplification of the arithmetic, consider the two ends of the diameter or of a chord to be at -1 and +1, and the breaks to be at -R and +R, as indicated in sketch (c). With

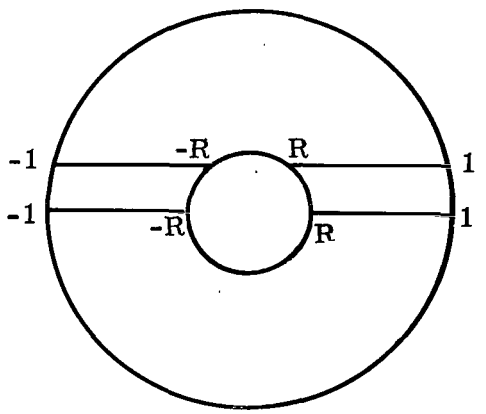

Sketch (c)

E in equation (1) equal to zero in the region between -R and +R, equation (2) now takes the following form:

$$2\pi D(x) = \pi\left[1 - 2\pi^2 m^2(x) + 2\int_{-1}^{-R}\frac{m(t)}{t-x}\,dt + 2\int_{R}^{1}\frac{m(t)}{t-x}\,dt\right]$$
$$+ i\left[-2\pi m(x) + \int_{-1}^{-R}\frac{dt}{t-x} + \int_{R}^{1}\frac{dt}{t-x} - 2\pi^2\int_{-1}^{-R}\frac{m^2(t)}{t-x}\,dt - 2\pi^2\int_{R}^{1}\frac{m^2(t)}{t-x}\,dt\right]$$

Multiplying both sides of the equation by their complex conjugates and retaining only the first-order terms in m gives the following equation for the intensity:

$$I(x) = 4\pi^2|D(x)|^2$$

$$= \pi^2\left[1 + 4\int_{-1}^{-R}\frac{m(t)}{t-x}\,dt + 4\int_{R}^{1}\frac{m(t)}{t-x}\,dt\right]$$
$$+ \ln^2\left|\frac{x+R}{x-R}\,\frac{1-x}{1+x}\right| - 4\pi^2 m(x)\,\ln\left|\frac{x+R}{x-R}\,\frac{1-x}{1+x}\right| \qquad (8)$$

Let $I_o(x)$ represent the intensity distribution for a perfect mirror (ref. 2),

$$I_o = \pi^2 + \ln^2 \left| \frac{x + R}{x - R} \frac{1 - x}{1 + x} \right|$$

Then

$$\frac{I(x) - I_o(x)}{4\pi^2} \equiv p(x) = \int_{-1}^{-R} \frac{m(t)}{t - x}\, dt + \int_{R}^{1} \frac{m(t)}{t - x}\, dt - m(x) \ln \left| \frac{x + R}{x - R} \frac{1 - x}{1 + x} \right| \tag{9}$$

The problem is to determine $m(x)$ along the two parts of the chord (that is, between -1 and -R, and between R and 1) when $p(x)$ is given along the same two parts. In the following section, some examples will be shown of $p(x)$ for several simple functions $m(x)$; and then the general method of solution will be developed, as before, in cosine series.

Examples of $p(x)$ Corresponding to Some Simple $m(x)$ Distributions

Example B-1.- If $m(x)$ is a constant, equation (9) gives $p(x) = 0$, as it should.

Example B-2.- If $m(x) = \frac{a}{x}$, where a is a constant,

$$p(x) = a \int_{-1}^{-R} \frac{dt}{t(t - x)} + a \int_{R}^{1} \frac{dt}{t(t - x)} - \frac{a}{x} \ln \left| \frac{x + R}{x - R} \frac{1 - x}{1 + x} \right| = 0$$

Thus, $m(x) = \text{Constant}$ and $m(x) = \frac{\text{Constant}}{x}$ are both solutions of the homogeneous integral equation, $p(x) = 0$. (The fact that $m(x) = \frac{\text{Constant}}{x}$ is a solution was first recognized by Dr. Gatewood.) The ambiguity introduced by these two solutions, and methods of overcoming it, are discussed in a later section.

Example B-3.- If $m(x) = x$,

$$p(x) = \int_{-1}^{-R} \frac{t\, dt}{t - x} + \int_{R}^{1} \frac{t\, dt}{t - x} - x \ln \left| \frac{x + R}{x - R} \frac{1 - x}{1 + x} \right| = 2(1 - R)$$

If $m(x)$ is x^2, x^3, . . ., then $p(x)$ is similarly easily evaluated. The first few p terms for these cases are listed in table VII, and four are plotted, together with the corresponding m terms, in figure 4. For all calculated examples, R was taken as 5/41, the same value that was used in reference 3. It will be seen that, in general, if $m(x)$ is symmetrical, $p(x)$ is antisymmetrical, and if $m(x)$ is antisymmetrical, p is symmetrical.

TABLE VII.- p(x) FOR $m(x) = x^n$; MIRROR WITH CENTRAL OBSCURATION

m(x)	p(x)
1	0
x	$2(1 - R)$
x^2	$2(1 - R)x$
x^3	$2\left[(1 - R)x^2 + \frac{1 - R^3}{3}\right]$
x^4	$2\left[(1 - R)x^3 + \frac{1 - R^3}{3}x\right]$
x^5	$2\left[(1 - R)x^4 + \frac{1 - R^3}{3}x^2 + \frac{1 - R^5}{5}\right]$

For the following three examples, and for the remainder of the discussion of the Cassegrain-mirror problem, it will be convenient to differentiate between the left- and right-hand sides of the mirror by means of the subscripts l and r.

Example B-4.- If $m_r(x) = +1$ and $m_l(x) = -1$,

$$p_l(x) = -\int_{-1}^{-R} \frac{dt}{t - x} + \int_{R}^{1} \frac{dt}{t - x} + \ln\left|\frac{x + R}{x - R}\frac{1 - x}{1 + x}\right| = 2 \ln\left|\frac{1 - x}{x - R}\right|$$

$$p_r(x) = -\int_{-1}^{-R} \frac{dt}{t - x} + \int_{R}^{1} \frac{dt}{t - x} - \ln\left|\frac{x + R}{x - R}\frac{1 - x}{1 + x}\right| = -2 \ln\left|\frac{x + R}{1 + x}\right|$$

It will be seen that these two expressions have the same value at symmetrically located points (that is, $p_r(x) = p_l(-x)$), as they should, since m is antisymmetrical.

Example B-5.- If $m_r(x) = x$ and $m_l(x) = -x$,

$$p_l(x) = -\int_{-1}^{-R} \frac{t\,dt}{t - x} + \int_{R}^{1} \frac{t\,dt}{t - x} + x \ln\left|\frac{x + R}{x - R}\frac{1 - x}{1 + x}\right|$$

$$= 2x \ln\left|\frac{1 - x}{x - R}\right|$$

Similarly,

$$p_r(x) = -2x \ln\left|\frac{x + R}{x + 1}\right|$$

In this case, $p_r(x) = -p_l(-x)$; that is, p is antisymmetrical, corresponding to the fact that m is symmetrical.

Example B-6.- An effort was made to find a function m(x) corresponding to $p_l = -1$, $p_r = +1$. No simple solution to this problem was found. However, by trial, a symmetrical function

$$m_r(x) = m_l(-x) = 0.94873|x| - 0.96455\sqrt{|x|} - 0.51652\,\frac{1}{\sqrt{|x|}} \tag{10}$$

was found that when substituted into equation (9), produced the desired p function to an accuracy of about 1 percent. Equation (10), of course, applies only for the case R = 5/41.

SOLUTION IN FOURIER SERIES; MIRROR WITH CENTRAL OBSCURATION

Decomposition of p(x) and m(x) Into Symmetrical and Antisymmetrical Parts

A function such as m(x) extending between -1 and +1 can always be decomposed into a symmetrical and an antisymmetrical part, where the symmetrical part is

$$m_s(x) = \frac{m_r(x) + m_l(-x)}{2}$$

and the antisymmetrical part is

$$m_a(x) = \frac{m_r(x) - m_l(-x)}{2}$$

where the subscripts s and a indicate "symmetrical" and "antisymmetrical," respectively. If the corresponding p(x) is similarly decomposed into symmetrical and antisymmetrical parts, p_s and p_a, inverting p_s will give m_a, and inverting p_a will give m_s; and the total solution will be, by the two preceding equations,

$$m_r(x) = m_s(x) + m_a(x)$$

$$m_l(x) = m_s(x) - m_a(x)$$

Solution for Antisymmetrical p, Symmetrical m

Development in power series in $\cos\phi$.- Given that $m_r(x) = m_l(-x)$, the first integral in equation (9) can be rewritten by substituting $t = -t$, as follows:

$$\int_{-1}^{-R} \frac{m_l(t)}{t - x}\,dt = \int_{1}^{R} \frac{m_l(-t)}{t + x}\,dt = -\int_{R}^{1} \frac{m_r(t)}{t + x}\,dt$$

Then equation (9) becomes

$$p_r(x) = \int_{R}^{1} m_r(t)\left(\frac{1}{t - x} - \frac{1}{t + x}\right)dt - m_r(x)\,\ln\left|\frac{x + R}{x - R}\,\frac{1 - x}{1 + x}\right|$$

$$= \int_{R}^{1}\left[m_r(t) - m_r(x)\right]\left(\frac{1}{t - x} - \frac{1}{t + x}\right)dt$$

$$= 2x\int_{R}^{1} \frac{m_r(t) - m_r(x)}{t^2 - x^2}\,dt \qquad (11)$$

With the substitution $x = \cos\phi$, $t = \cos\theta$, the results shown in table VIII are readily derived for $m_r(\phi) = \cos^2\phi, \cos^4\phi, \cos^6\phi, \ldots$. The subscript r is not used for the column headings in the table, since the table actually applies to both the left and right sides; however, the subscripts s and a are used, since they are pertinent.

TABLE VIII.- $p(\phi)$ FOR $m(\phi) = \cos^{2n}\phi$; MIRROR WITH CENTRAL OBSCURATION

$m_s(\phi)$	$p_a(\phi)$
$\cos^2\phi$	$2(1 - R)\cos\phi$
$\cos^4\phi$	$2\left[(1 - R)\cos^3\phi + \frac{1 - R^3}{3}\cos\phi\right]$
$\cos^6\phi$	$2\left[(1 - R)\cos^5\phi + \frac{1 - R^3}{3}\cos^3\phi + \frac{1 - R^5}{5}\cos\phi\right]$
.	.
.	.
.	.

This table may be inverted just as table IV was inverted to form table V. However, because of the various powers of R that occur in the coefficients, the procedure that

was used for the simple mirror would have involved a burdensome amount of algebra. Instead, the table was set up in a recursive form, in which each line is determined from the preceding lines. This formulation is shown in table IX.

By use of the formulas for $\cos n\theta$ ($\cos 3\theta = 4\cos^3\theta - 3\cos\theta$, $\cos 5\theta = 16\cos^5\theta - 20\cos^3\theta + 5\cos\theta$, and so forth; see equation (7) for the general formula), the lines of table IX can be grouped to give table X. If now the antisymmetrical part of $p(\phi)$ is analyzed into a Fourier series of the form $a_1\cos\phi + a_3\cos 3\phi + a_5\cos 5\phi + \ldots$, the corresponding symmetrical part of $m(\phi)$ is found directly by using table X.

TABLE IX.- $m(\phi)$ FOR $p(\phi) = \cos^{2n+1}\phi$; MIRROR WITH CENTRAL OBSCURATION

$p_a(\phi)$	$m_s(\phi)$
$\cos\phi$	$\frac{1}{2(1-R)}\cos^2\phi \equiv M_1$
$\cos^3\phi$	$\frac{1}{2(1-R)}\left[\cos^4\phi - \frac{2}{3}(1-R^3)M_1\right] \equiv M_3$
$\cos^5\phi$	$\frac{1}{2(1-R)}\left[\cos^6\phi - \frac{2}{3}(1-R^3)M_3 - \frac{2}{5}(1-R^5)M_1\right] \equiv M_5$
.	.
.	.
.	.

TABLE X.- $m(\phi)$ FOR $p(\phi) = \cos(2n+1)\phi$; MIRROR WITH CENTRAL OBSCURATION

$p_a(\phi)$	$m_s(\phi)$
$\cos\phi$	M_1
$\cos 3\phi$	$4M_3 - 3M_1$
$\cos 5\phi$	$16M_5 - 20M_3 + 5M_1$
.	.
.	.
.	.

The procedure is essentially similar to what was described for the simple mirror, except that the m terms remain as powers of $\cos \phi$. It is described in more detail after the following remark.

Remark on the Fourier analysis.- The function p_a is defined only between $x = R$ and $x = 1$ (or between $\phi = \cos^{-1}R$ and $\phi = 0$). In order to determine the coefficients of its Fourier series in the usual manner, however, p_a will also have to be defined for values of ϕ that fall within the obscuration – that is, for ϕ between $\pi/2$ and $\cos^{-1}R$. If a large number of terms are used in the Fourier series, this additional section of the p_a distribution may, presumably, be chosen arbitrarily, since the series is required to represent p_a only on the actual mirror. However, it would be reasonable to choose this additional section so that it forms a smooth continuation of the given p_a curve, in order that the p_a curve be represented as accurately as possible by a given number of Fourier terms.

In the problems to be discussed later, nine-term Fourier series were used to represent p_a and p_s, and of the nine points (at $\phi = 5^o, 15^o, 25^o, \ldots, 85^o$) that were used in the Fourier analysis, only the innermost one, at $\phi = 85^o$, was within the central obscuration $\left(\text{between } \phi = \frac{\pi}{2} \text{ and } \phi = \cos^{-1}R\right)$. For all but one of the problems, p_a and p_s were given by continuous analytical expressions; hence, the values of these expressions at $\phi = 85^o$ were used for the innermost point as the obvious best choice, with excellent results. In the final problem, $p_a = 1$ (that is, $p_r = 1$, $p_l = -1$), the p curve has too violent a break between the right and left side to yield a very smooth m curve. This problem is discussed separately, and a simple method of handling such cases is suggested.

Inversion matrix for antisymmetrical p, symmetrical m.- As in the procedure for the simple mirror, the first step is to determine the coefficients for a cosine series that represents p_a. A nine-term series was used in the present work. The procedure is essentially as follows:

(1) Locate nine points along the mirror semidiameter or semichord at $x = \cos 5^o$, $x = \cos 15^o$, $x = \cos 25^o, \ldots,$ $x = \cos 85^o$. The values of p_a at these nine points, arranged in a column, is the vector $\{p_a\}$.

(2) Prepare a 9×9 Fourier-analysis matrix $[F_a]$. The product $[F_a]\{p_a\}$ is a vector whose elements are the nine desired Fourier coefficients. As with the simple mirror, this step was not actually performed.

$$\left[F_a\right] \equiv \begin{bmatrix} \frac{\cos 5^o}{4.5} & \frac{\cos 15^o}{4.5} & \frac{\cos 25^o}{4.5} & \cdots & \frac{\cos 85^o}{4.5} \\ \frac{\cos 15^o}{4.5} & \frac{\cos 45^o}{4.5} & \frac{\cos 75^o}{4.5} & \cdots & \frac{\cos 255^o}{4.5} \\ \frac{\cos 25^o}{4.5} & \frac{\cos 75^o}{4.5} & \frac{\cos 125^o}{4.5} & \cdots & \frac{\cos 425^o}{4.5} \\ \vdots & \vdots & \vdots & \vdots & \vdots \\ \frac{\cos 85^o}{4.5} & \frac{\cos 255^o}{4.5} & \frac{\cos 425^o}{4.5} & \cdots & \frac{\cos 1445^o}{4.5} \end{bmatrix}$$

3. By use of the formulas in table IX, calculate $M_1 = \frac{1}{2(1 - R)} \cos^2\phi$, $M_3 = \frac{1}{2(1 - R)}\left[\cos^4\phi - \frac{2}{3}(1 - R^3)M_1\right]$, etc., for the nine values of ϕ and the given value of R. Arrange in a 9×9 matrix $\left[M_s\right]$ as shown.

$$\left[M_s\right] \equiv \begin{bmatrix} M_1(5^o) & M_3(5^o) & M_5(5^o) & \cdots & M_{17}(5^o) \\ M_1(15^o) & M_3(15^o) & M_5(15^o) & \cdots & M_{17}(15^o) \\ M_1(25^o) & M_3(25^o) & M_5(25^o) & \cdots & M_{17}(25^o) \\ \vdots & \vdots & \vdots & \vdots & \vdots \\ M_1(85^o) & M_3(85^o) & M_5(85^o) & \cdots & M_{17}(85^o) \end{bmatrix}$$

(4) Set up a 9×9 matrix $\left[C_s\right]$ whose elements are the coefficients in table X. The coefficients in each line of the table, in reversed order, form the elements of one of the columns in $\left[C_s\right]$. This matrix is given completely.

$$[C_s] \equiv \begin{bmatrix} 1 & -3 & 5 & -7 & 9 & -11 & 13 & -15 & 17 \\ 0 & 4 & -20 & 56 & -120 & 220 & -364 & 560 & -816 \\ 0 & 0 & 16 & -112 & 432 & -1232 & 2912 & -6048 & 11\,424 \\ 0 & 0 & 0 & 64 & -576 & 2816 & -9984 & 28\,800 & -71\,808 \\ 0 & 0 & 0 & 0 & 256 & -2816 & 16\,640 & -70\,400 & 239\,360 \\ 0 & 0 & 0 & 0 & 0 & 1024 & -13\,312 & 92\,160 & -452\,608 \\ 0 & 0 & 0 & 0 & 0 & 0 & 4096 & -61\,440 & 487\,424 \\ 0 & 0 & 0 & 0 & 0 & 0 & 0 & 16\,384 & -278\,528 \\ 0 & 0 & 0 & 0 & 0 & 0 & 0 & 0 & 65\,536 \end{bmatrix}$$

It will be seen that the product $[M_s][C_s]$ is a matrix whose ij element is the contribution of the (unit) jth cosine at the ith point. For example, the element at the third row and fifth column is the value of m_s at $\phi = 25^o$ (the third point) corresponding to $p_a = \cos 9\phi$ (the fifth cosine, see table X). Multiplying the vector of Fourier coefficients, given by $[F_a]\{p_a\}$, by this matrix $[M_s][C_s]$ will now give the nine elements of $\{m_s\}$ (that is, the values of m_s at $\phi = 5^o, 15^o, 25^o, \ldots, 85^o$). Thus,

$$\{m_s\} = [M_s][C_s][F_a]\{p_a\}$$

The complete inversion matrix $[M_s][C_s][F_a]$ is given in the appendix. Multiplying the vector $\{p_a\}$ by this matrix will give $\{m_s\}$.

Solution for Symmetrical p, Antisymmetrical m

Given that $m_r(x) = -m_l(-x)$, the same procedure as before provides the equation

$$p_r(x) = \int_R^1 m_r(t)\left(\frac{1}{t-x} + \frac{1}{t+x}\right)dt - m_r(x)\ln\left|\frac{R+x}{x-R}\frac{1-x}{1+x}\right|$$

$$= \int_R^1 \left[\frac{m_r(t) - m_r(x)}{t-x} + \frac{m_r(t) + m_r(x)}{t+x}\right]dt$$

$$= 2\int_R^1 \frac{tm_r(t) - xm_r(x)}{t^2 - x^2}\,dt \qquad (12)$$

(Incidentally, it is obvious from this equation that $m(x) = \frac{\text{Constant}}{x}$ is a solution of the homogeneous equation $p(x) = 0$. (See example B-2.)) Letting $m_r(x)$ be x, x^3, x^5, . . . (or letting $m_r(\phi)$ be $\cos\phi$, $\cos^3\phi$, $\cos^5\phi$, . . .) and proceeding as before yields eventually the relations shown in table XI, which corresponds to table IX, presented previously for the case of antisymmetrical p, symmetrical m.

TABLE XI.- $m(\phi)$ FOR $p(\phi) = \cos^{2n}\phi$; MIRROR WITH CENTRAL OBSCURATION

$p_s(\phi)$	$m_a(\phi)$
1	$\frac{1}{2(1 - R)} \cos\phi \equiv M_0$
$\cos^2\phi$	$\frac{1}{2(1 - R)}\left[\cos^3\phi - \frac{2}{3}(1 - R^3)M_0\right] \equiv M_2$
$\cos^4\phi$	$\frac{1}{2(1 - R)}\left[\cos^5\phi - \frac{2}{3}(1 - R^3)M_2 - \frac{2}{5}(1 - R^5)M_0\right] \equiv M_4$
.	.
.	.
.	.

There is an obvious relationship between the M terms in this table and those in table IX; namely, $M_1 = M_0 \cos\phi$, $M_3 = M_2 \cos\phi$, $M_5 = M_4 \cos\phi$, ...

The procedure now follows the same pattern as before. The steps are

(1) Find the values of the symmetrical part of p, that is, p_s, at the nine points $\phi = 5^o, 15^o, 25^o, \ldots, 85^o$, and arrange them in a column vector $\{p\}$.

(2) Prepare a 9×9 Fourier matrix $[F_s]$ as shown, such that, when $\{p_s\}$ is multiplied by it, the components of the product vector will be the coefficients of the series $a_o + a_2 \cos 2\phi + a_4 \cos 4\phi + \ldots + a_{16} \cos 16\phi$ that equals p_s at these nine points.

$$\left[F_s\right] \equiv \begin{bmatrix} \frac{1}{9} & \frac{1}{9} & \frac{1}{9} & \cdots & \frac{1}{9} \\ \frac{\cos 10^\circ}{4.5} & \frac{\cos 30^\circ}{4.5} & \frac{\cos 50^\circ}{4.5} & \cdots & \frac{\cos 170^\circ}{4.5} \\ \frac{\cos 20^\circ}{4.5} & \frac{\cos 60^\circ}{4.5} & \frac{\cos 100^\circ}{4.5} & \cdots & \frac{\cos 340^\circ}{4.5} \\ \vdots & \vdots & \vdots & \vdots & \vdots \\ \frac{\cos 80^\circ}{4.5} & \frac{\cos 240^\circ}{4.5} & \frac{\cos 400^\circ}{4.5} & \cdots & \frac{\cos 1360^\circ}{4.5} \end{bmatrix}$$

(3) Set up a 9×9 matrix $\left[M_a\right]$ as shown, by using the formulas of table XI.

$$\left[M_a\right] = \begin{bmatrix} M_0(5^\circ) & M_2(5^\circ) & M_4(5^\circ) & \cdots & M_{16}(5^\circ) \\ M_0(15^\circ) & M_2(15^\circ) & M_4(15^\circ) & \cdots & M_{16}(15^\circ) \\ M_0(25^\circ) & M_2(25^\circ) & M_4(25^\circ) & \cdots & M_{16}(25^\circ) \\ \vdots & \vdots & \vdots & \vdots & \vdots \\ M_0(85^\circ) & M_2(85^\circ) & M_4(85^\circ) & \cdots & M_{16}(85^\circ) \end{bmatrix}$$

As mentioned previously, every term in the matrix $\left[M_s\right]$ is $\cos \phi$ times the corresponding term in this matrix $\left[M_a\right]$.

(4) Set up a 9×9 matrix $\left[C_a\right]$ whose elements are the coefficients in the expansion of $\cos n\phi$ in powers of $\cos \phi$ ($\cos 0 = 1$, $\cos 2\phi = 2 \cos^2\phi - 1$, $\cos 4\phi = 8 \cos^4\phi - 8 \cos^2\phi + 1$, and so forth. (See eq. (7).) This matrix is here given completely.

$$[C_a] = \begin{bmatrix} 1 & -1 & 1 & -1 & 1 & -1 & 1 & -1 & 1 \\ 0 & 2 & -8 & 18 & -32 & 50 & -72 & 98 & -128 \\ 0 & 0 & 8 & -48 & 160 & -400 & 840 & -1568 & 2688 \\ 0 & 0 & 0 & 32 & -256 & 1120 & -3584 & 9408 & -21\,504 \\ 0 & 0 & 0 & 0 & 128 & -1280 & 6912 & -26\,880 & 84\,480 \\ 0 & 0 & 0 & 0 & 0 & 512 & -6144 & 39\,424 & -180\,224 \\ 0 & 0 & 0 & 0 & 0 & 0 & 2048 & -28\,672 & 212\,992 \\ 0 & 0 & 0 & 0 & 0 & 0 & 0 & 8192 & -131\,072 \\ 0 & 0 & 0 & 0 & 0 & 0 & 0 & 0 & 32\,768 \end{bmatrix}$$

Finally,

$$\{m_a\} = [M_a][C_a][F_s]\{p_s\}$$

The complete inversion matrix $[M_a][C_a][F_s]$ is given in the appendix. Multiplying vector $\{p_s\}$ by this matrix will give $\{m_a\}$.

Example Problems

Problems B-1 to B-4.- Four simple cases were calculated in order to verify the general correctness of the approach and also to verify the numerical accuracy of the two inversion matrices $[M_s][C_s][F_a]$ and $[M_a][C_a][F_s]$. The assumed p functions, which were either symmetrical or antisymmetrical, are listed in the following table, together with the corresponding m functions:

p(x)	m(x)
1	$\frac{x}{2(1 - R)}$
$2(1 - R)x$	x^2
$2\left[(1 - R)x^2 + \frac{1 - R^3}{3}\right]$	x^3
$2\left[(1 - R)x^3 + \frac{1 - R^3}{3}x\right]$	x^4

In these four cases, when x is replaced by $\cos\phi$, both $m(\phi)$ and $p(\phi)$ are expressible in terms of a constant, $\cos\phi$, $\cos 2\phi$, $\cos 3\phi$, and $\cos 4\phi$. Hence, they are expressible exactly by the nine-term Fourier series, and the calculated values of m should be exactly correct, as in fact they were. These four examples are shown in the four upper parts of figure 4. In all calculations, R was taken as 5/41, the same value that was used in reference 3.

Problem B-5.- In this problem, for antisymmetrical p, p_r was assumed to be $2x \ln \frac{1+x}{R+x}$. This p_r corresponds to the case $m_r = x$, $m_l = -x$, which was discussed earlier. Unlike the p terms of the preceding four cases, this p_r is not expressible exactly in terms of a few $\cos n\phi$ terms. However, its plot is a very smooth curve, which approaches the origin smoothly (fig. 4(e)). The computed values of m_r fell very accurately on a straight line (the line designated "m" in figure 4(e)). Accordingly, the points are not shown. The ticks on the curves of figure 4(e) (which have been omitted from the curves of figures 4(a) to 4(d) because of the small scale) indicate the x locations of the p and m points.

It may be noted that the calculated m_r line is somewhat below the line $m_r = x$. As noted previously, $m(x)$ can be determined (and need be defined) only to within a constant. Accordingly, the difference is of no consequence.

Problem B-6.- In this problem, also for antisymmetrical p, p_r was assumed to be a constant, 1 (with $p_l = -1$). As mentioned earlier, a reasonably accurate, but not exact, solution to this problem has been found in the form of the following algebraic expression:

$$m_r(x) = m_l(-x) = 0.94873|x| - 0.96455\sqrt{|x|} - 0.51652\,\frac{1}{\sqrt{|x|}} \tag{10}$$

The nine values of m_r found by the Fourier analysis method are shown by the circled points in figure 5. The upper line is a plot of the preceding algebraic expression for m_r, with a constant added in order to provide a best fit. The scatter of the points about the line reflects the inadequacy of the nine-term cosine series in representing a p_r curve that has a fairly abrupt irregularity. Nevertheless, on the whole, the fit seems to be fairly good.

A second calculation was made in which the sharpness of the irregularity was somewhat alleviated by slightly reducing the value of p_r for the one point that falls within the obscuration. For this case, the elements of the vector $\{p\}$ were taken as 1,1,1,1,1,1,1, 1, and 0.9 (see the sketch in fig. 5). The calculated result is shown by the square symbols in the figure; and the line through them is a plot of the algebraic expression for m_r with

a different constant added to provide a best fit. On the whole, the fit seems to be somewhat improved, with reduced scatter of the points about the line.

A third calculation was made in which the elements of $\{p\}$ were taken as 1,1,1,1, 1,1,1,1,1, and 0.7. (See the sketch in fig. 5.) Although the sketch now shows a definite deviation of the p curve from the straight line in the region just outside the obscuration, the calculated m_r points (triangles) showed very good agreement with the true curve (the bottom curve of fig. 5).

It appears from this example that the present method will provide a reasonably satisfactory solution even in the case of a fairly abrupt change in the value of p across the obscuration. Judiciously choosing the p values within the obscuration can reduce the sharpness of the break and improve the results.

Increasing the number of points (and the number of cosine terms in the series) will improve the accuracy. Another approach is to decompose p_a into two parts, one of which is smooth and the other of which is like this problem, and use equation (10) as the solution of the latter part.

Problem B-7.- The final problem is the same as that used in reference 3. It is a bump that is identical in size, shape, and radial location with the bump of problem A-3 for the simple mirror. It is shown together with the corresponding p function in figure 6. The p function in this case is given by the equations

$$p(x) = -2z^3 + \frac{10}{3}z - (1 - z^2) \ln \left| \frac{1 - z}{1 + z} \frac{1 + x}{1 - x} \frac{x - R}{x + R} \right| \qquad (z^2 \leq 1)$$

$$p(x) = -2z^3 + \frac{10}{3}z - (1 - z^2)^2 \ln \left| \frac{z - 1}{z + 1} \right| \qquad (z^2 \geq 1)$$

where

$$z = \frac{x - 0.6}{0.2} = 5x - 3$$

The first step in the analysis is to decompose p into a symmetrical and an antisymmetrical part. The method has been described previously; table XII shows the arithmetic. The table also shows the nine values of m_s calculated from the nine values of p_a and the nine values of m_a calculated from the nine values of p_s. The last two columns list the m values that represent the final solution.

This solution is plotted in figure 6. It is generally closer to the true solution (the original bump) than was the first result for the simple mirror, where the calculation used only six points on each side; but it is not quite as close as was the second result for the simple mirror, where 12 points were used on each side.

TABLE XII.- STEPS IN DECOMPOSING p AND COMPOSING m; EXAMPLE B-7

ϕ, deg	x ($\cos\phi$)	$p_r(x)$	$p_l(-x)$	p_s $\left(\frac{p_r + p_l}{2}\right)$	p_a $\left(\frac{p_r - p_l}{2}\right)$	m_a	m_s	$m_r(x)$ $(m_s + m_a)$	$m_l(-x)$ $(m_s - m_a)$
5	0.99619	0.55995	-0.13395	0.21300	0.34695	-0.00192	-0.00632	-0.00824	-0.00440
15	.96593	.61076	-.13655	.23710	.37366	.00820	.00728	.01548	-.00092
25	.90631	.74645	-.14199	.30223	.44422	-.01098	-.01781	-.02879	-.00683
35	.81915	1.14548	-.15075	.49737	.64812	.01144	.01226	.02370	.00082
45	.70711	1.36675	-.16376	.60149	.76525	-.24742	-.25694	-.50436	-.00952
55	.57358	-1.53599	-.18254	-.85926	-.67672	-.45945	-.45735	-.91680	.00210
65	.42262	-1.70324	-.20977	-.95651	-.74679	-.06215	-.07554	-.13769	-.01339
75	.25882	-.66017	-.25036	-.45527	-.20490	.00653	.00643	.01296	-.00010
85	.08716	-.42551	-.31433	-.36992	-.05559	.02349	-.00122	.02227	-.02471

The additive constant.- In the earlier case of the simple mirror, the solutions for m were always obtained in such a form that the average value of m (averaged with respect to ϕ) was zero. That is, whatever may have been the original m function, when it was rederived from the corresponding p function, an additive constant had been introduced such that its average value was zero.

In the present solution for the Cassegrain-type mirror, a different condition is imposed, namely, that the solution pass through the origin. That is, whatever may have been the original m function, when it is rederived from the corresponding p function, an additive constant has been introduced such that $m = 0$ at $x = 0$. The reason will be apparent on referring to table IX or table XI, where it can be seen that all the M terms contain $\cos\phi$ as a factor and are therefore zero at $\phi = 90^\circ$ ($x = 0$). In further clarification of this matter, consider, for example, M_1 in table IX, which is listed as $\frac{1}{2(1 - R)}\cos^2\phi$. Since a constant may be added without affecting the relation between p and m, M_1 might also have been given as $\frac{1}{2(1 - R)}\left(\cos\phi - \frac{1}{2}\right) = \frac{\cos 2\phi}{4(1 - R)}$, in which case its average value would have been zero. In the case of the simple mirror, all the M terms were actually written in this manner – that is, in terms of $\cos n\phi$ – so that the average value of every M was zero. In the case of the Cassegrain-type mirror, however, the M terms are all in terms of $\cos^n\phi$, and the average is zero only when n is odd (as in table XI).

NOTES ON APPLICATION OF METHOD

Survey of Complete Mirror Surface

Simple mirror.- The analysis in this paper has been concerned with the mirror-surface distortion along the diameter or any chord that is normal to the knife-edge. In

order to survey the entire mirror surface, many chords and/or diameters must be examined. Some care must be exercised, however, in selecting the set of chords and diameters.

Consider first the case of the simple mirror. With a fixed knife-edge setting, one could study all chords normal to the knife-edge and thereby cover the entire mirror. However, even if all these chords appeared to be perfect, one could not conclude that the mirror was perfect. As previously pointed out, one could conclude only that all these chords were perfect parabolas with their foci on the knife-edge. Additional data would be required in order to establish that the mirror is a perfect paraboloid of revolution. For example, one could rotate the knife edge through 90^{o} and examine the diameter, which now intersects the complete set of chords that were tested with the previous knife-edge setting. (See sketch (d).) If this diameter also turns out to be a parabola with its focus on the knife edge, the perfection of the mirror would be established. Or, if the mirror has imperfections, the data for the set of parallel chords combined with the data for this diameter are sufficient to analyze the mirror surface completely.

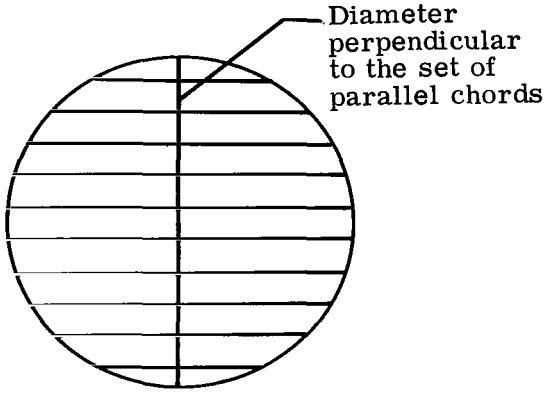

Sketch (d)

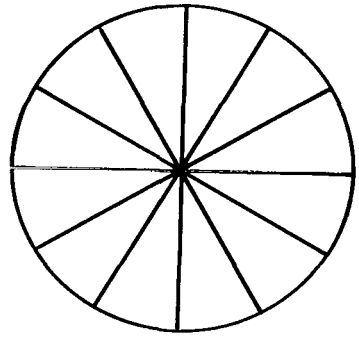

Sketch (e)

An alternative approach is to rotate the knife-edge through a series of small steps and study only the diameter for each knife-edge setting. (See sketch (e).) If all the diameters are found to be perfect parabolas with the same focal point, the fact that all the vertexes coincide (since all the parabolas pass through the center point of the mirror) would establish that the mirror is a perfect paraboloid of revolution. Or, if any one of the diameters shows an imperfection, the imperfection may be evaluated quantitatively relative to an exact parabola that passes through the common vertex (the center point of the mirror), which serves as the common reference point. This method seems preferable to that of the preceding paragraph, because it can use a single row of sensors with fixed spacing.

Cassegrain mirror.- For the Cassegrain mirror, the fact that the central area of the mirror is obscured makes it impossible to use the center point of the mirror as a common reference point. Accordingly, the method of the preceding paragraph is not sufficient to show whether the mirror is a perfect paraboloid of revolution – every diameter could be a perfect parabola with its focus on the knife edge, yet the vertexes of all these parabolas need not coincide.

Some point located outside the obscuration will have to serve as a reference point, and all parabolas either (1) must pass through this point or (2) must be more or less indirectly referable to this point. The left-hand sketch (sketch (f)) shows the first approach, in which all the parabolas pass through the common reference point, P. It will be recalled, however, that any analysis of a parabola that passes through the obscuration may be in error by $\Delta m(x) = \frac{\text{Constant}}{x}$, where the constant is arbitrary. Accordingly, this approach seems to be not quite adequate, since some of the parabolas pass through the obscuration, as shown in sketch (f).

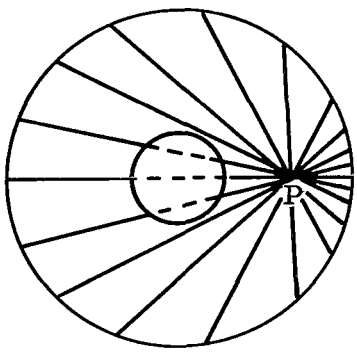

Sketch (f)

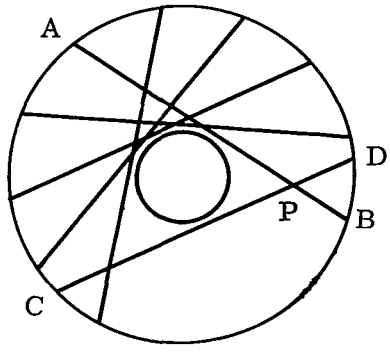

Sketch (g)

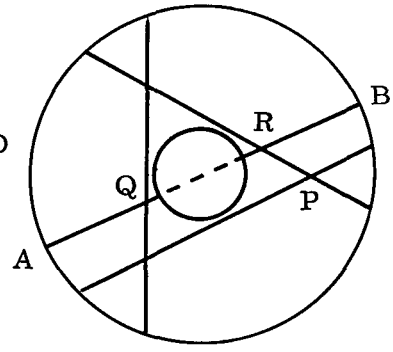

Sketch (h)

The method indicated in the middle sketch (sketch (g)), in which the mirror is covered with a set of equal unbroken parabolas, avoids this difficulty. Every one of the indicated family of parabolas cuts at least one of the two parabolas AB and CD through P, and can thus be referred to P. This procedure has the additional advantage that all the test chords have the same length, so that a single row of sensors with fixed spacing can be used for the entire survey.

The method of the preceding paragraph avoids having to deal with the case of a broken parabola – that is, a parabola that passes through the obscuration. The possible error $\Delta m(x) = \frac{\text{Constant}}{x}$, however, may generally exist to only a negligible extent; and it may be unrealistic to forego using any broken parabolas for a reason that could be more theoretical than real. In any case, a combination of broken and unbroken parabolas can be arranged for which the analysis of the mirror surface would provide a unique answer.

Such a combination is indicated in the right-hand sketch (sketch (h)). For the three unbroken parabolas the errors, if any, can be determined at every point relative to the point P, as discussed in the preceding paragraph. Specifically, the errors at points Q and R are known, and hence the difference between the errors at points Q and R is known. If analysis of the broken parabola AB provides a different value for this difference, the discrepancy determines the constant in the extraneous solution $\Delta m(x) = \frac{\text{Constant}}{x}$ that has to be removed. The entire mirror surface can thus be analyzed by means of broken parabolas passing through the center, all checked against the initial set of three unbroken parabolas.

Optical Theory

Cassegrain arrangement.- A mirror with a central obscuration would typically be used with a secondary mirror near its focus; the secondary mirror reflects the converging beam back through the hole to the instrument chambers. The effect of the secondary mirror has not been considered in this study, where it has been assumed that the knife-edge is simply at the focus of the primary mirror. Some study is needed to assess the effect of the secondary mirror on the applicability of the present theory to determining distortions of the primary mirror. Study is also needed to determine whether the effects of small errors in the secondary mirror can be analyzed as if they were due to errors in the primary mirror, and the errors then compensated for by distorting the primary mirror. (From a cursory examination of this question, it would appear that, in general, complete compensation is unlikely. Although the compensation may cause the light from an on-axis star to come to a sharp focus, the compensation would hardly apply for the light from off-axis stars; hence, in general, the width of the field would be reduced, unless the error in the secondary mirror was very small and gradual.)

Diffraction theory.- There are some approximations in the development in reference 1; however, they seem to be of quite minor significance if the total ratio is fairly large. One assumption, of uncertain significance, is that the knife-edge does not affect the part of the wave front that does not impinge on it. This assumption has been of concern in the past where it has been applied in diffraction theory; and its validity may be especially questionable in the present case, where the entire Airy disk is only a few wavelengths in diameter. In any case, some experimental quantitative verification of the basic theory of reference 2 is desirable.

Decomposition of p and m for the Simple Mirror

In the analysis for the mirror with the central obscuration, p was decomposed into a symmetric part p_s and an antisymmetric part p_a, and m was then found in the

corresponding two parts which then had to be combined. This procedure had the advantage that two 9 × 9 matrices had to be developed and used instead of one 18 × 18 matrix, which would have been more troublesome. It should be pointed out that this procedure is directly adaptable to the simple mirror case. That is, the 12 × 12 matrix that was developed could have been replaced with two 6 × 6 matrices. The procedure for developing this pair of matrices is a fairly obvious modification of the procedure that was used for developing the 12 × 12 matrix. Alternatively, the procedure that was used for developing the two 9 × 9 matrices for the mirror with the central obscuration may be applied directly to the case of the simple mirror. One has only to put R equal to zero in tables IX and XI and recalculate the elements of the $[M_a]$ and $[M_s]$ matrices. The $[C_a]$ and $[C_s]$ matrices, and the $[F_a]$ and $[F_s]$ matrices may be used without modification.

The Nonlinear Problem

Equations (4) and (5) were derived from equation (1) under the assumption that the error in the mirror surface was no more than about one-twentieth of a wavelength. Results calculated by the exact equation in references 2 and 3 show that as the error in the mirror surface increases, the effects on the diffraction pattern quickly acquire a different character and are not even recognizable as extrapolations of the small-error effects. For such cases, experienced opticians can, by observing the pattern as they move the knife-edge in the focal plane, locate the error and estimate its magnitude. The technique can possibly be adapted for an orbiting telescope, so that it might generally be possible to reduce a large error by successive applications of relatively coarse corrections until the error is sufficiently small to be determined exactly by the small-error theory.

One may hope that the problem of reducing large errors would exist only during the initial adjustment of the telescope after launch, and that with adequate thermal control of the telescope, the errors that develop subsequently will remain within the range that can be analyzed by the linear theory. In any case, a reasonably practical method of solving the nonlinearized problem, or, at least, of taking into account the second-order terms that were deleted from equation (3) would be very desirable.

Color

It has been tacitly assumed throughout the present analysis and discussion that the light is monochromatic – that is, that the starlight is filtered through a fairly narrow band-pass filter. Actually, for a perfect mirror, the diffraction pattern (see fig. 1) is independent of wavelength. If the mirror is not perfect, however, the deviation p from the ideal intensity distribution of figure 1 is proportional to the error m (see eq. (5)),

where m is measured in half-wavelengths. For a given imperfection, then, m will be greater for blue light than for red light, and the intensity increment p will accordingly be greater for blue light than for red light. It follows that use of a blue filter will maximize the sensitivity of the knife-edge test.

On the other hand, if the imperfection in the mirror figure is large, the present linearized theory might not be very applicable if blue light is used (see the preceding section), but it might remain satisfactory if red or infrared is used (since the imperfection will then be smaller in terms of half-wavelengths). Thus, the longer wavelengths should be used for analyzing large errors in the mirror figure, but the shorter wavelengths will provide increased sensitivity after the error has been reduced.

CONCLUDING REMARKS

It appears from the present work and the work of Gatewood that Linfoot's integral equation for the light intensity distribution in the knife-edge pattern can be readily inverted to determine errors in the primary optics of a telescope, provided the errors are small. This approach to determining the errors seems practical and furthermore requires no special apparatus in the main telescope tube or special treatment of the mirror (as are required in other suggested approaches). Nevertheless, many details of the procedure remain to be studied. Some of these details have been discussed in the last section of the present paper.

Laboratory studies of the method will be needed to identify problem areas and to indicate practical experimental approaches to obtaining the basic data.

Langley Research Center,
National Aeronautics and Space Administration,
Hampton, Va., March 29, 1971.

APPENDIX

MATRICES USED IN ANALYSIS

This appendix contains the four inversion matrices that were used for the calculated examples of the present paper. They are applicable to 12-point and 24-point analyses of the simple mirror and to 18-point analyses of the mirror with a central obscuration (Cassegrain type). As was mentioned in the main text, the number of significant figures shown is doubtless excessive.

The printouts that are here reproduced are only six columns wide; accordingly, each matrix row requires at least two rows of the printout. Thus, in the 12×12 matrix, the first row of the printout, reading from left to right, contains the first six elements of the matrix row; and the second row of the printout, reading from left to right, contains the seventh to the twelfth elements.

12 × 12 INVERSION MATRIX $[M][F]$ FOR SIMPLE MIRROR

ROW 1					
1.58827075E-01	9.49552840E-02	2.40752492E-02	4.84739143E-02	2.21414808E-02	3.51095584E-02
2.01664358E-02	2.71101263E-02	1.79946258E-02	2.03809443E-02	1.49855264E-02	1.15022107E-02
ROW 2					
-4.77232344E-02	1.66533159E-01	1.32233825E-01	1.27709820E-02	5.84097441E-02	1.43423129E-02
3.93341090E-02	1.46342319E-02	2.82655304E-02	1.39090034E-02	1.90056322E-02	1.02244713E-02
ROW 3					
-2.92248554E-03	-1.04385188E-01	1.54173409E-01	1.61999662E-01	9.31196557E-03	6.39332915E-02
1.13390435E-02	3.98861057E-02	1.24393883E-02	2.59310534E-02	1.25159659E-02	1.24544588E-02
ROW 4					
-2.03274109E-02	-2.58694095E-03	-1.44210995E-01	1.22214951E-01	1.85651400E-01	6.49648338E-03
6.72888099E-02	8.83556405E-03	3.88865613E-02	1.03592036E-02	2.23813914E-02	9.39169660E-03
ROW 5					
-6.68016357E-03	-4.03997174E-02	-1.90380095E-03	-1.74884789E-01	7.87160958E-02	1.99043574E-01
5.18765253E-03	6.62841225E-02	7.87504673E-03	3.43213263E-02	1.01439120E-02	1.36384568E-02
ROW 6					
-1.56198543E-02	-7.18292143E-03	-5.28422274E-02	-3.03531918E-03	-1.93896871E-01	2.68506993E-02
2.02459869E-01	3.58366475E-03	6.20782485E-02	6.62392926E-03	2.79012469E-02	8.34263162E-03
ROW 7					
-8.34263161E-03	-2.79012469E-02	-6.62392925E-03	-6.20782486E-02	-3.58366478E-03	-2.02459869E-01
-2.68506993E-02	1.93896871E-01	3.03531918E-03	5.28422274E-02	7.18292144E-03	1.56198543E-02
ROW 8					
-1.36384568E-02	-1.01439119E-02	-3.43213263E-02	-7.87504674E-03	-6.62841225E-02	-5.18765250E-03
-1.99043574E-01	-7.87160958E-02	1.74884789E-01	1.90380094E-03	4.03997174E-02	6.68016357E-03
ROW 9					
-9.39169659E-03	-2.23813914E-02	-1.03592037E-02	-3.88865613E-02	-8.83556403E-03	-6.72888100E-02
-6.49648336E-03	-1.85651400E-01	-1.22214951E-01	1.44210995E-01	2.58694095E-03	2.03274109E-02
ROW 10					
-1.24544588E-02	-1.25159659E-02	-2.59310534E-02	-1.24393883E-02	-3.98861057E-02	-1.13390435E-02
-6.39332915E-02	-9.31196556E-03	-1.61999662E-01	-1.54173409E-01	1.04385188E-01	2.92248555E-03
ROW 11					
-1.02260812E-02	-1.90068107E-02	-1.39094348E-02	-2.82650990E-02	-1.46330533E-02	-3.93324991E-02
-1.43407030E-02	-5.84085656E-02	-1.27705507E-02	-1.32234256E-01	-1.66534337E-01	4.77216245E-02
ROW 12					
-1.15022107E-02	-1.49855264E-02	-2.03809444E-02	-1.79946258E-02	-2.71101263E-02	-2.01664358E-02
-3.51095584E-02	-2.21414808E-02	-4.84739143E-02	-2.40752492E-02	-9.49552840E-02	-1.58827075E-01

24 × 24 INVERSION [M][F] MATRIX FOR SIMPLE MIRROR

ROW 1						
1.36227046E-01	6.62340205E-02	1.60970652E-02	3.39613915E-02	1.45984833E-02	2.53715160E-02
1.34470894E-02	2.09345679E-02	1.25220957E-02	1.80364514E-02	1.17274715E-02	1.58738865E-02
1.10019563E-02	1.41028747E-02	1.03006239E-02	1.25388574E-02	9.58198162E-03	1.10563932E-02
8.79465651E-03	9.53475388E-03	7.85003443E-03	7.77355182E-03	6.51071174E-03	4.85198124E-03
ROW 2						
-2.90306796E-02	1.53868939E-01	8.77568805E-02	8.76927227E-03	4.06131449E-02	9.42754998E-03
2.92912665E-02	9.54597783E-03	2.36080428E-02	9.45658284E-03	1.99421683E-02	9.26034216E-03
1.72272107E-02	8.98906479E-03	1.50163365E-02	8.64456724E-03	1.30731192E-02	8.20626729E-03
1.12381395E-02	7.61871309E-03	9.35606375E-03	6.72645978E-03	7.14388681E-03	4.64334420E-03
ROW 3						
-1.18983071E-04	-6.34986658E-02	1.62523356E-01	1.06912210E-01	6.62197315E-03	4.56471843E-02
7.41519808E-03	3.18558516E-02	7.79707474E-03	2.51412418E-02	7.96553586E-03	2.08730335E-02
8.00084099E-03	1.77314273E-02	7.93474654E-03	1.51739826E-02	7.77167829E-03	1.29132411E-02
7.49045124E-03	1.07437333E-02	7.02439196E-03	8.41546916E-03	6.15416626E-03	4.97592573E-03
ROW 4						
-1.07219561E-02	5.09056917E-04	-8.90318288E-02	1.62221895E-01	1.25745869E-01	5.02404965E-03
5.07866267E-02	5.88248521E-03	3.44215795E-02	6.40897394E-03	2.66162330E-02	6.73563036E-03
2.17184996E-02	6.92299536E-03	1.81413814E-02	6.99483119E-03	1.52407672E-02	6.94730944E-03
1.26773006E-02	6.73885911E-03	1.02039783E-02	6.22681632E-03	7.48589687E-03	4.53912092E-03
ROW 5						
-2.24782096E-03	-2.27914277E-02	1.01936214E-03	-1.11829231E-01	1.56281148E-01	1.42819297E-01
4.17771031E-03	5.52257884E-02	4.98616343E-03	3.64480075E-02	5.55387656E-03	2.76136312E-02
5.96046962E-03	2.21166702E-02	6.24526321E-03	1.81150454E-02	6.42179928E-03	1.48614238E-02
6.47833227E-03	1.19494619E-02	6.35832270E-03	9.02801452E-03	5.85465149E-03	5.08884652E-03
ROW 6						
-7.82327601E-03	-1.74290103E-03	-3.16521881E-02	7.10000285E-04	-1.31724976E-01	1.45043889E-01
1.58417997E-01	3.36015520E-03	5.92777224E-02	4.15396383E-03	3.82395583E-02	4.75827707E-03
2.84290058E-02	5.22594541E-03	2.23631784E-02	5.58166397E-03	1.79626554E-02	5.82631373E-03
1.43846316E-02	5.92555988E-03	1.11640525E-02	5.74691536E-03	7.85756183E-03	4.43419770E-03
ROW 7						
-3.08196174E-03	-1.52794522E-02	-1.04406642E-03	-3.96699966E-02	6.63246210E-04	-1.49562970E-01
1.29844603E-01	1.71819574E-01	2.87184701E-03	6.24757239E-02	3.63168524E-03	3.94261673E-02
4.25357830E-03	2.87352427E-02	4.77052372E-03	2.21410588E-02	5.19655324E-03	1.73465295E-02
5.52457516E-03	1.34056765E-02	5.70655557E-03	9.73522982E-03	5.54944609E-03	5.21353873E-03
ROW 8						
-6.72042437E-03	-2.98715125E-03	-2.05693919E-02	-1.10571482E-03	-4.63069365E-02	3.17077527E-04
-1.64813510E-01	1.10943441E-01	1.83166392E-01	2.32062809E-03	6.50496959E-02	3.07151792E-03
4.02498795E-02	3.71586193E-03	2.87869939E-02	4.27448975E-03	2.17290729E-02	4.75020908E-03
1.65916654E-02	5.11533531E-03	1.23419350E-02	5.24970756E-03	8.29434092E-03	4.32000251E-03
ROW 9						
-3.53319880E-03	-1.22336000E-02	-2.37637105E-03	-2.54522135E-02	-9.88378048E-04	-5.22507697E-02
1.70195860E-04	-1.77784924E-01	8.93448613E-02	1.91932867E-01	1.98187855E-03	6.66413320E-02
2.72508679E-03	4.03975373E-02	3.39762908E-03	2.82787122E-02	4.01289368E-03	2.07978829E-02
4.56886178E-03	1.52984840E-02	5.02789998E-03	1.06092050E-02	5.21792004E-03	5.36073205E-03
ROW 10						
-6.14581806E-03	-3.79665664E-03	-1.59350214E-02	-2.41556427E-03	-2.93154357E-02	-1.20572235E-03
-5.70571000E-02	-1.69969763E-04	-1.88008500E-01	6.53587176E-02	1.98259798E-01	1.55103035E-03
6.74758683E-02	2.30093986E-03	4.01161121E-02	3.00372278E-03	2.74845958E-02	3.66519248E-03
1.96695627E-02	4.26700859E-03	1.38825552E-02	4.70723635E-03	8.83866508E-03	4.18861621E-03
ROW 11						
-3.82235965E-03	-1.05936229E-02	-3.33699777E-03	-1.94112740E-02	-2.27357680E-03	-3.27858531E-02
-1.27011419E-03	-6.11129117E-02	-3.54959688E-04	-1.95696945E-01	3.99134796E-02	2.01746350E-01
1.28887057E-03	6.72469534E-02	2.05924595E-03	3.91085418E-02	2.81628662E-03	2.60816049E-02
3.56559612E-03	1.79476825E-02	4.28663696E-03	1.17588392E-02	4.83884683E-03	5.54484213E-03
ROW 12						
-5.79047771E-03	-4.38194588E-03	-1.33872353E-02	-3.43815311E-03	-2.20310433E-02	-2.46640413E-03
-3.54341156E-02	-1.55545923E-03	-6.40615920E-02	-7.00139678E-04	-2.00478559E-01	1.33671648E-02
2.02587096E-01	9.17328200E-04	6.62040386E-02	1.71525348E-03	3.76531728E-02	2.52347991E-03
2.43952615E-02	3.33824959E-03	1.60500961E-02	4.08611809E-03	9.56049878E-03	4.02894191E-03

24 × 24 INVERSION [M][F] MATRIX FOR SIMPLE MIRROR – Concluded

ROW 13					
-4.02894191E-03	-9.56049878E-03	-4.08611809E-03	-1.60500961E-02	-3.33824959E-03	-2.43952515E-02
-2.52347991E-03	-3.76531728E-02	-1.71525348E-03	-6.62040386E-02	-9.17328200E-04	-2.02587096E-01
-1.33671648E-02	2.00478559E-01	7.00139678E-04	6.40615920E-02	1.55545923E-03	3.54341156E-02
2.46640413E-03	2.20310433E-02	3.43815311E-03	1.33872353E-02	4.38194588E-03	5.79047771E-03
ROW 14					
-5.54484213E-03	-4.83884683E-03	-1.17588392E-02	-4.28663696E-03	-1.79476825E-02	-3.56559612E-03
-2.60816049E-02	-2.81628662E-03	-3.91085418E-02	-2.05924595E-03	-6.72469534E-02	-1.28887057E-03
-2.01746350E-01	-3.99134796E-02	1.95696945E-01	3.54959688E-04	6.11129117E-02	1.27011419E-03
3.27858531E-02	2.27357680E-03	1.94112740E-02	3.33699777E-03	1.05936229E-02	3.82235965E-03
ROW 15					
-4.18861621E-03	-8.83866508E-03	-4.70723635E-03	-1.38825552E-02	-4.26700859E-03	-1.96695627E-02
-3.66519248E-03	-7.74845958E-02	-3.00372278E-03	-4.01161121E-02	-2.30093986E-03	-6.74758683E-02
-1.55103035E-03	-1.98259798E-01	-6.53587176E-02	1.88008500E-01	1.69969763E-04	5.70571000E-02
1.20572235E-03	2.83154357E-02	2.41566427E-03	1.59350214E-02	3.79665664E-03	6.14581806E-03
ROW 16					
-5.36073205E-03	-5.21792004E-03	-1.06092050E-02	-5.02789998E-03	-1.52984840E-02	-4.56868178E-03
-2.07978829E-02	-4.01289368E-03	-2.82787122E-02	-3.39762908E-03	-4.03975373E-02	-2.72508679E-03
-6.66413320E-02	-1.98187855E-03	-1.91932867E-01	-8.93448613E-02	1.77784924E-01	-1.70195860E-04
5.22507697E-02	9.88378048E-04	2.54522135E-02	2.37637105E-03	1.22336000E-02	3.53319880E-03
ROW 17					
-4.32000251E-03	-8.29434092E-03	-5.24970756E-03	-1.23419350E-02	-5.11533531E-03	-1.65916654E-02
-4.75020908E-03	-2.17290779E-02	-4.27448975E-03	-2.87869939E-02	-3.71586193E-03	-4.02498795E-02
-3.07151792E-03	-6.50496959E-02	-2.32062809E-03	-1.83166392E-01	-1.10943441E-01	1.64813510E-01
-3.17077527E-04	4.63069365E-02	1.10571482E-03	2.05693919E-02	2.98715125E-03	6.72042437E-03
ROW 18					
-5.21353873E-03	-5.54944609E-03	-9.73522982E-03	-5.70655557E-03	-1.34056765E-02	-5.52457516E-03
-1.73465295E-02	-5.19655324E-03	-2.21410588E-02	-4.77052372E-03	-2.87352427E-02	-4.25357830E-03
-3.94261673E-02	-3.63168524E-03	-6.24757239E-02	-2.87184701E-03	-1.71819574E-01	-1.29844603E-01
1.49562970E-01	-6.63246210E-04	3.96699966E-02	1.04406642E-03	1.52794522E-02	3.08196174E-03
ROW 19					
-4.43419770E-03	-7.85756183E-03	-5.74691536E-03	-1.11640525E-02	-5.92555988E-03	-1.43846316E-02
-5.82631373E-03	-1.79626554E-02	-5.58166397E-03	-2.23631784E-02	-5.22594541E-03	-2.84290058E-02
-4.75827707E-03	-3.82395583E-02	-4.15396383E-03	-5.92777224E-02	-3.36015520E-03	-1.58417997E-01
-1.45043889E-01	1.31724976E-01	-7.10000285E-04	3.16521881E-02	1.74290103E-03	7.82327601E-03
ROW 20					
-5.08894652E-03	-5.85465149E-03	-9.02801452E-03	-6.35832270E-03	-1.19494619E-02	-6.47833227E-03
-1.48614238E-02	-6.42179928E-03	-1.81150454E-02	-6.24526321E-03	-2.21166702E-02	-5.96046962E-03
-2.76136312E-02	-5.55387656E-03	-3.64480075E-02	-4.98616343E-03	-5.52257884E-02	-4.17771031E-03
-1.42819297E-01	-1.56281148E-01	1.11829231E-01	-1.01936214E-03	2.27914277E-02	2.24782096E-03
ROW 21					
-4.53912092E-03	-7.48589687E-03	-6.22681632E-03	-1.02039783E-02	-6.73885911E-03	-1.26773006E-02
-6.94730944E-03	-1.52407672E-02	-6.99483119E-03	-1.81413814E-02	-6.92299536E-03	-2.17164996E-02
-6.73563036E-03	-2.66162330E-02	-6.40897394E-03	-3.44215795E-02	-5.88248521E-03	-5.07866267E-02
-5.02404965E-03	-1.25745869E-01	-1.62221895E-01	8.90318288E-02	-5.09056917E-04	1.07219561E-02
ROW 22					
-4.97592573E-03	-6.15416626E-03	-8.41546916E-03	-7.02439196E-03	-1.07437333E-02	-7.49045124E-03
-1.29132411E-02	-7.77167829E-03	-1.51739826E-02	-7.93476654E-03	-1.77314273E-02	-8.00084099E-03
-2.08730335E-02	-7.96553586E-03	-2.51412418E-02	-7.79707474E-03	-3.18558516E-02	-7.41519808E-03
-4.56471843E-02	-6.62197315E-03	-1.06912210E-01	-1.62523356E-01	6.34986658E-02	1.18983071E-04
ROW 23					
-4.64334420E-03	-7.14388681E-03	-6.72645978E-03	-9.35606375E-03	-7.61871309E-03	-1.12381395E-02
-8.20626729E-03	-1.30731192E-02	-8.64456724E-03	-1.50163365E-02	-8.98904479E-03	-1.72272107E-02
-9.26034216E-03	-1.99421683E-02	-9.45658284E-03	-2.36080428E-02	-9.54597783E-03	-2.92912665E-02
-9.42754998E-03	-4.06131449E-02	-8.76927227E-03	-8.77568805E-02	-1.53868939E-01	2.90306796E-02
ROW 24					
-4.85198124E-03	-6.51071174E-03	-7.77351582E-03	-7.85003443E-03	-9.53475388E-03	-8.79465651E-03
-1.10563932E-02	-9.58198162E-03	-1.25388574E-02	-1.03006239E-02	-1.41028747E-02	-1.10019563E-02
-1.58738865E-02	-1.17274715E-02	-1.80364514E-02	-1.25220957E-02	-2.09345679E-02	-1.34470894E-02
-2.53715160E-02	-1.45984833E-02	-3.39613915E-02	-1.60970652E-02	-6.62340205E-02	-1.36227046E-01

9×9 INVERSION MATRIX $[M_s][C_s][F_a]$ FOR ANTISYMMETRICAL p, SYMMETRICAL m.

MIRROR WITH CENTRAL OBSCURATION, R = 5/41.

ROW 1					
1.57811803E-01	9.33846612E-02	4.05208065E-02	6.07500224E-02	5.92879902E-02	6.09486835E-02
1.20362791E-01	3.97740311E-02	1.06904775E+00			
ROW 2					
-2.95647649E-02	1.73403820E-01	1.34646196E-01	2.59563586E-02	9.62841761E-02	3.56134190E-02
1.46271233E-01	1.74876098E-02	1.09126029E+00			
ROW 3					
6.91653853E-03	-7.25948690E-02	1.81527792E-01	1.59221076E-01	4.53238759E-02	9.05423483E-02
1.06991123E-01	5.77587354E-02	1.05415448E+00			
ROW 4					
-6.24153969E-03	8.42345343E-03	-9.58374232E-02	1.60510341E-01	2.10596142E-01	2.48104787E-02
1.76864790E-01	4.39612621E-03	1.10757345E+00			
ROW 5					
3.68179232E-03	-1.88863744E-02	1.64895529E-02	-1.27290994E-01	1.55178876E-01	2.18765202E-01
9.48936157E-02	8.92280726E-02	1.03514744E+00			
ROW 6					
-2.14975995E-03	3.96771461E-03	-1.87096935E-02	8.51756562E-03	-1.24254270E-01	9.59834435E-02
3.14541900E-01	-1.37556354E-02	1.13665916E+00			
ROW 7					
2.08315033E-03	-7.99628756E-03	1.08483925E-02	-2.97937008E-02	2.64467798E-02	-1.54340971E-01
1.09167461E-01	2.27672566E-01	9.94678914E-01			
ROW 8					
-2.42245572E-04	3.36424653E-04	-2.06092978E-03	2.60604003E-04	-8.75115131E-03	-2.37526055E-03
-8.01195643E-02	-1.04009902E-01	1.23969337E+00			
ROW 9					
7.15900144E-04	-2.30826048E-03	4.13569866E-03	-7.21909222E-03	1.11625908E-02	-2.15804235E-02
3.84866309E-02	-1.36305501E-01	3.61485147E-01			

9 × 9 INVERSION MATRIX $[M_a][C_a][F_s]$ FOR SYMMETRICAL p, ANTISYMMETRICAL m.

MIRROR WITH CENTRAL OBSCURATION, R = 5/41.

ROW 1

1.57811803E-01	9.05472156E-02	3.68646034E-02	4.99535936E-02	4.20830787E-02	3.50922653E-02
5.10618191E-02	1.03335992E-02	9.35295586E-02			

ROW 2

-3.04912253E-02	1.73403820E-01	1.26335680E-01	2.20122536E-02	7.04849089E-02	2.11476051E-02
6.39975582E-02	4.68579091E-03	9.84647045E-02			

ROW 3

7.60251551E-03	-7.73702486E-02	1.81527792E-01	1.43909466E-01	3.53619603E-02	5.73016786E-02
4.98907800E-02	1.64944635E-02	1.01373527E-01			

ROW 4

-7.59051850E-03	9.93274847E-03	-1.06034287E-01	1.60510341E-01	1.81790379E-01	1.73724842E-02
9.12483714E-02	1.38899878E-03	1.17843064E-01			

ROW 5

5.18702703E-03	-2.57992572E-02	2.11348704E-02	-1.47461006E-01	1.55178876E-01	1.77453488E-01
5.67153024E-02	3.26597413E-02	1.27588996E-01			

ROW 6

-3.73372986E-03	6.68179125E-03	-2.95631756E-02	1.21643444E-02	-1.53181043E-01	9.59834435E-02
2.31758389E-01	-6.20705489E-03	1.72715951E-01			

ROW 7

4.91039670E-03	-1.82761167E-02	2.32644528E-02	-5.77485005E-02	4.42496197E-02	-2.09471176E-01
1.09167461E-01	1.39430786E-01	2.05130699E-01			

ROW 8

-9.32403389E-04	1.25555390E-03	-7.21676685E-03	8.24801367E-04	-2.39085900E-02	-5.26388421E-03
-1.30824959E-01	-1.04009902E-01	4.17459217E-01			

ROW 9

8.18277609E-03	-2.55818876E-02	4.30059545E-02	-6.78501952E-02	9.05636665E-02	-1.42021879E-01
1.86621702E-01	-4.04774930E-01	3.61485147E-01			

REFERENCES

1. Robertson, Hugh J.: Development of an Active Optics Concept Using a Thin Deformable Mirror. NASA CR-1593, 1970.

2. Linfoot, E. H.: Recent Advances in Optics. Clarendon Press (Oxford), 1958.

3. Gatewood, B. E.: Comparison of Various Methods of Mathematical Analysis of the Foucault Knife-Edge Test Pattern to Determine Optical Imperfections. NASA CR-1906, 1971.

4. Adams, Edwin P.; and Hippisley, R. L.: Smithsonian Mathematical Formulae and Tables of Elliptic Functions. First reprint, Smithsonian Misc. Collect., vol. 74, no. 1, 1939.

5. Garrick, I. E.: Conformal Mapping in Aerodynamics, With Emphasis on the Method of Successive Conjugates. Construction and Applications of Conformal Maps, Appl. Math. Series 18, National Bur. Standards, Dec. 26, 1952, pp. 137-147.

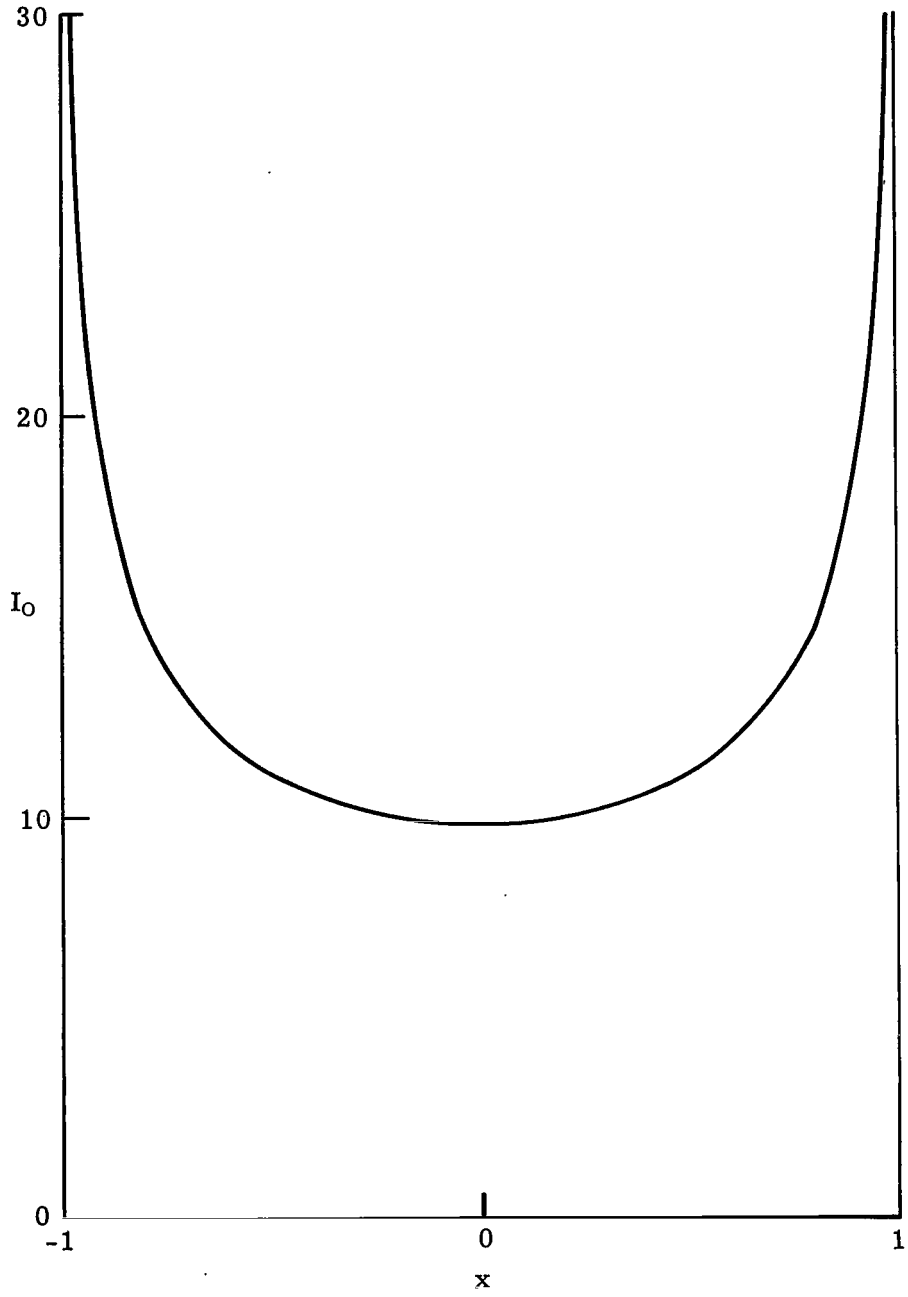

Figure 1.- Chordwise intensity distribution I_o for a perfect mirror.

$$I_o = \pi^2 + \ln^2\left(\frac{1 - x}{1 + x}\right).$$

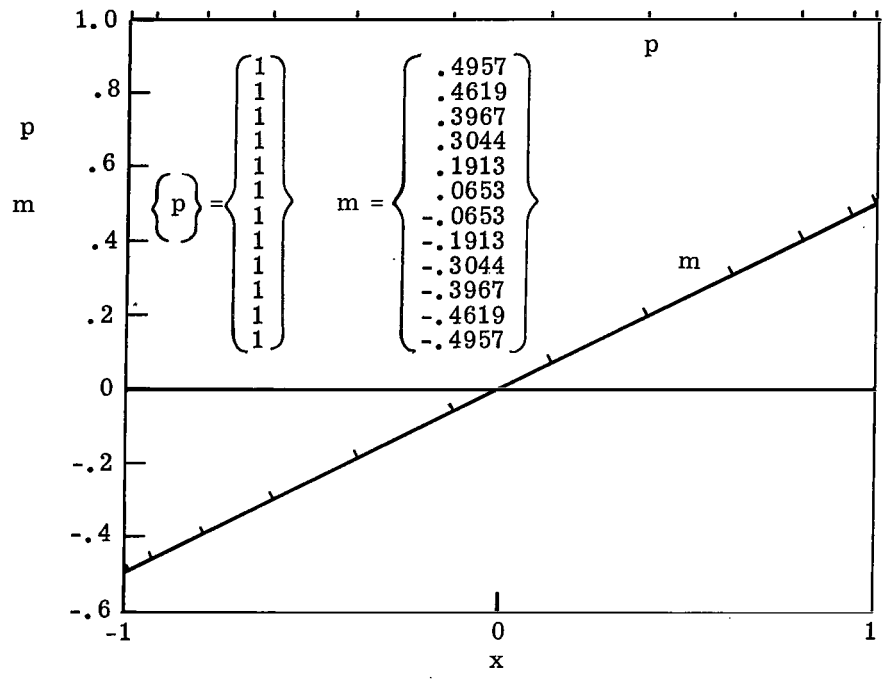

(a) $p = 1$; $m = \frac{1}{2}x$.

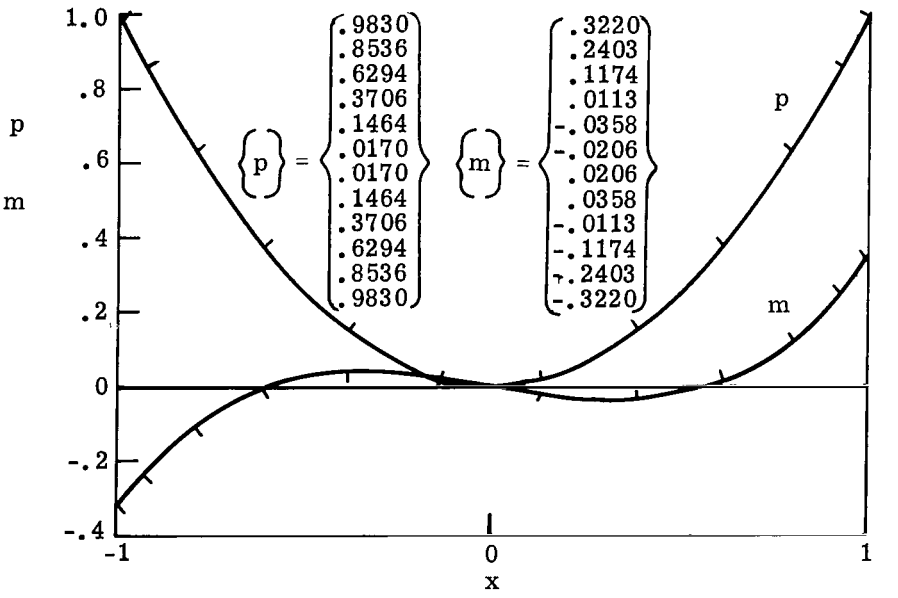

(b) $p = x^2$; $m = \frac{1}{2}\left(x^3 - \frac{x}{3}\right)$.

Figure 2.- Simple examples for the plain mirror. Ticks show the input p points and the calculated m points.

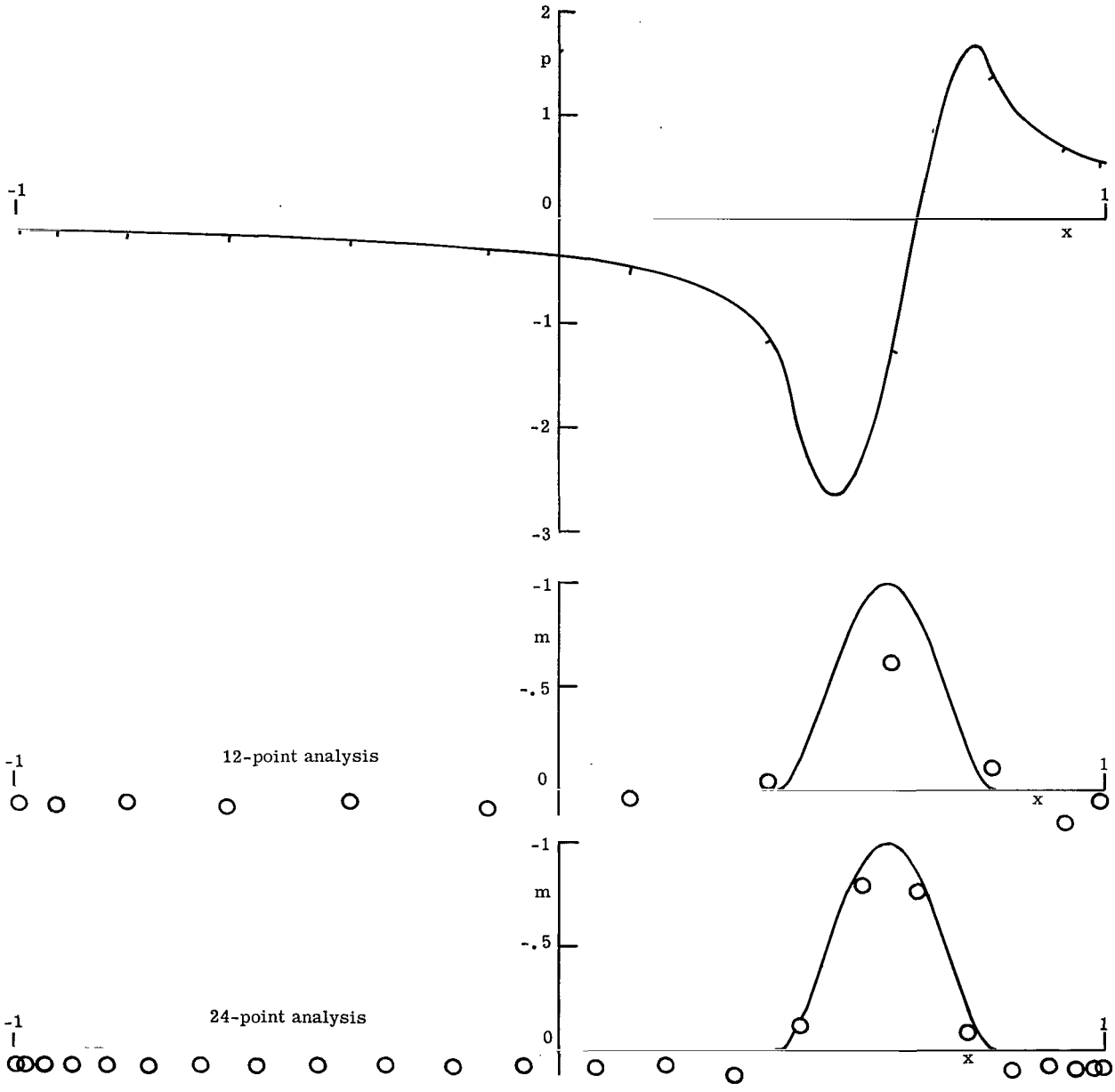

Figure 3.- Bump at x = 0.6 on simple mirror. Circled points show results calculated by 12-point analysis and by 24-point analysis. Ticks on upper curve show input p values for 12-point analysis.

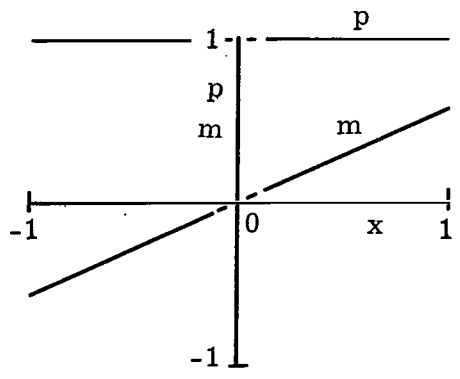

(a) $p = 1$; $m = \frac{x}{2(1 - R)}$.

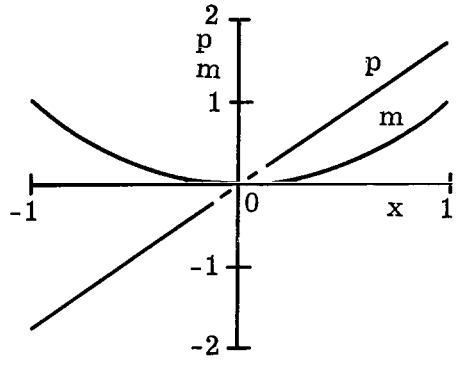

(b) $p = 2(1 - R)x$; $m = x^2$.

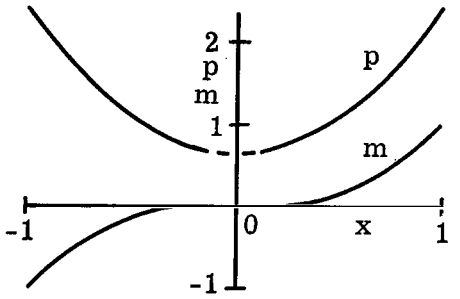

(c) $p = 2\left[(1 - R)x^2 + \frac{1}{3}(1 - R^3)\right]$; $m = x^3$.

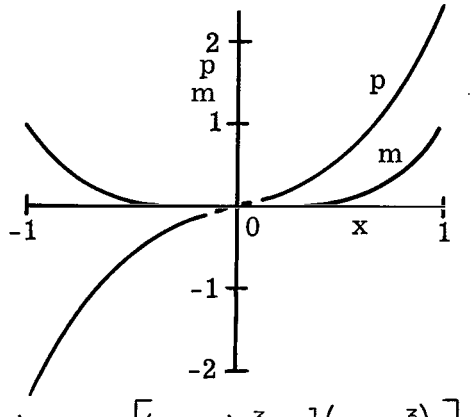

(d) $p = 2\left[(1 - R)x^3 + \frac{1}{3}(1 - R^3)x\right]$; $m = x^4$.

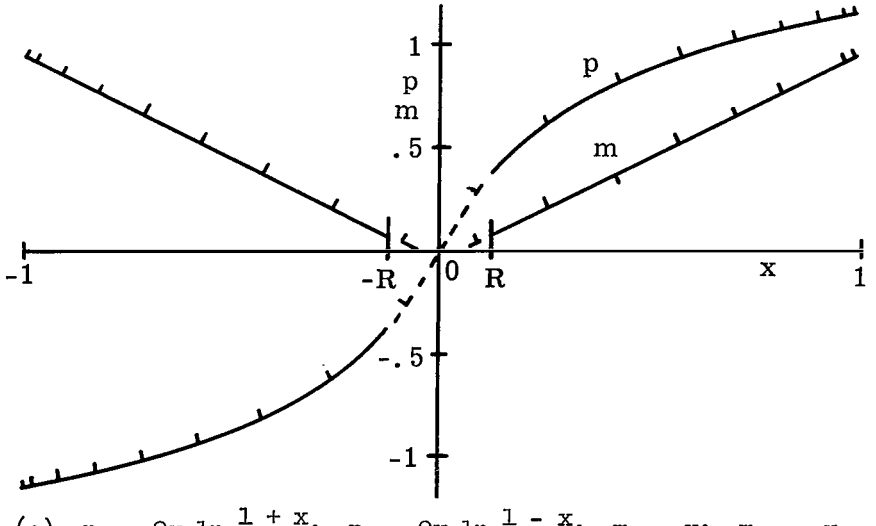

(e) $p_r = 2x \ln \frac{1 + x}{R + x}$; $p_l = 2x \ln \frac{1 - x}{R - x}$; $m_r = x$; $m_l = -x$.

Figure 4.- Simple examples for the mirror with a central obscuration. $R = 5/41$.

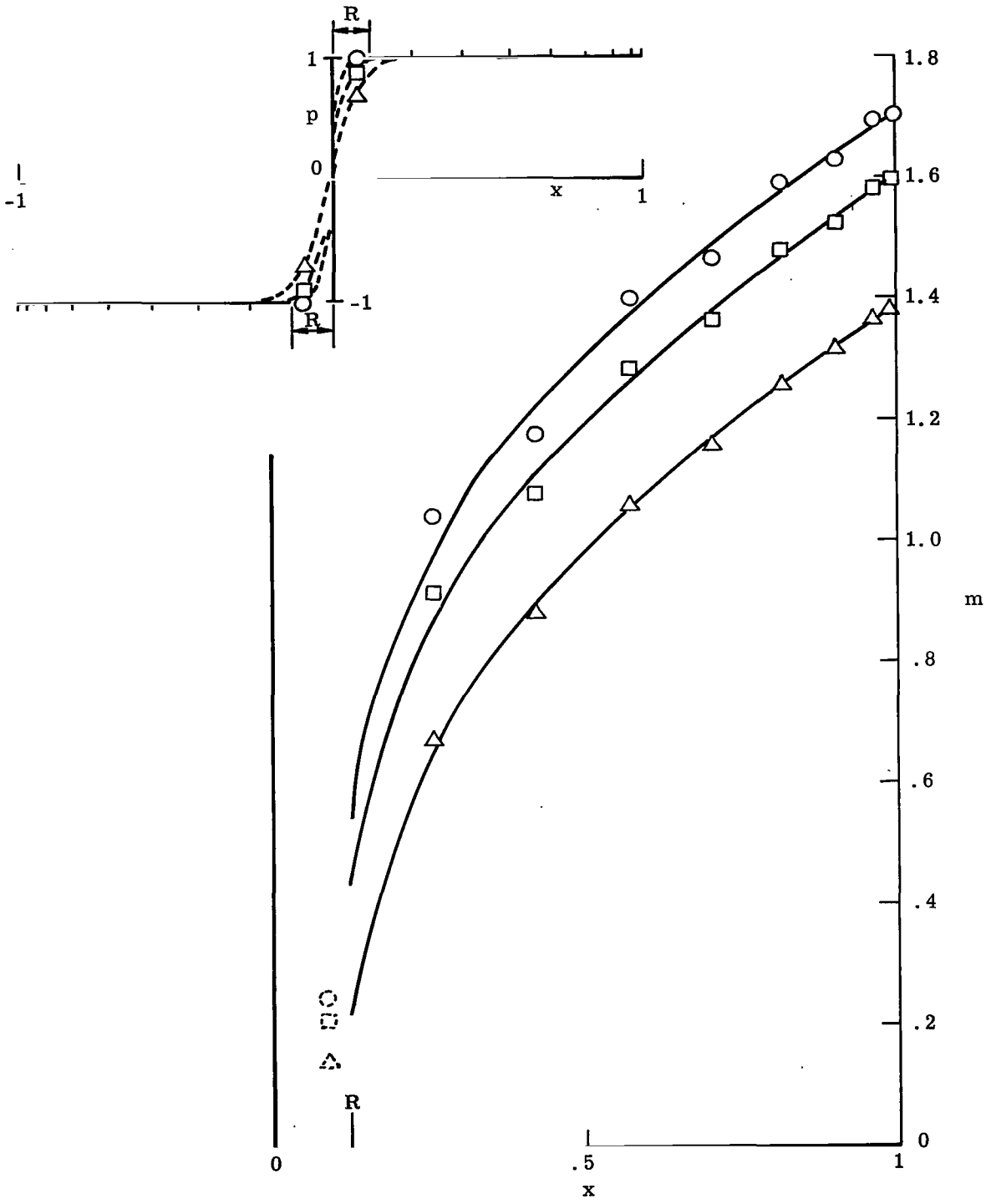

Figure 5.- Example of a sharp change in p across the central obscuration. $p_r = 1$; $p_l = -1$. The curves represent $m = 0.94873|x| - 0.96455\sqrt{|x|} - 0.51652\frac{1}{\sqrt{|x|}} +$ a constant. The sketch shows the three assumed p distributions.

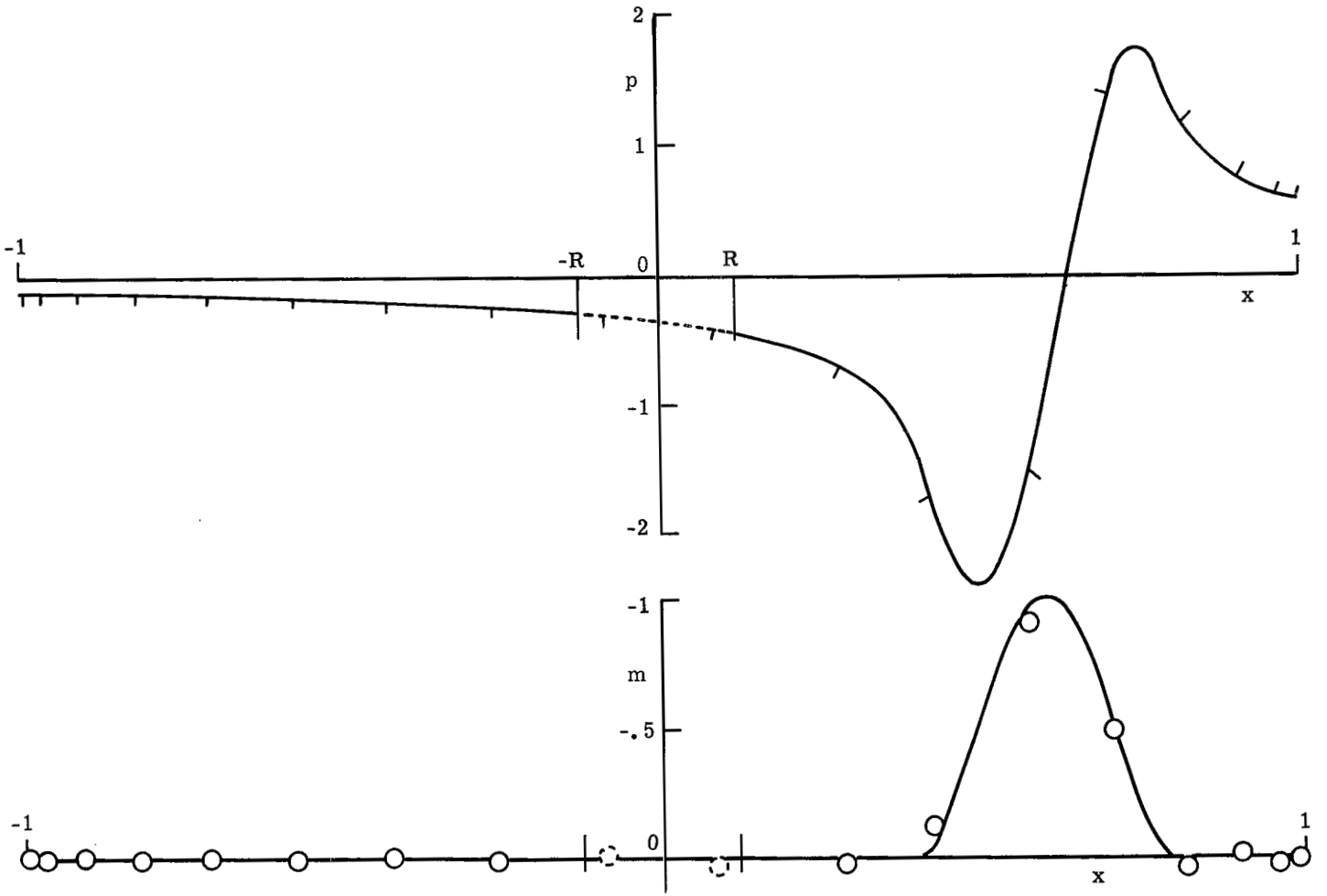

Figure 6.- Example of the bump at x = 0.6 on the mirror with a central obscuration. R = 5/41.

006 001 C1 U 14 710730 S00903DS
DEPT OF THE AIR FORCE
WEAPONS LABORATORY /WLOL/
ATTN: E LOU BOWMAN, CHIEF TECH LIBRARY
KIRTLAND AFB NM 87117

"The aeronautical and space activities of the United States shall be conducted so as to contribute . . . to the expansion of human knowledge of phenomena in the atmosphere and space. The Administration shall provide for the widest practicable and appropriate dissemination of information concerning its activities and the results thereof."

—NATIONAL AERONAUTICS AND SPACE ACT OF 1958

NASA SCIENTIFIC AND TECHNICAL PUBLICATIONS

TECHNICAL REPORTS: Scientific and technical information considered important, complete, and a lasting contribution to existing knowledge.

TECHNICAL NOTES: Information less broad in scope but nevertheless of importance as a contribution to existing knowledge.

TECHNICAL MEMORANDUMS: Information receiving limited distribution because of preliminary data, security classification, or other reasons.

CONTRACTOR REPORTS: Scientific and technical information generated under a NASA contract or grant and considered an important contribution to existing knowledge.

TECHNICAL TRANSLATIONS: Information published in a foreign language considered to merit NASA distribution in English.

SPECIAL PUBLICATIONS: Information derived from or of value to NASA activities. Publications include conference proceedings, monographs, data compilations, handbooks, sourcebooks, and special bibliographies.

TECHNOLOGY UTILIZATION PUBLICATIONS: Information on technology used by NASA that may be of particular interest in commercial and other non-aerospace applications. Publications include Tech Briefs, Technology Utilization Reports and Technology Surveys.

Details on the availability of these publications may be obtained from:

SCIENTIFIC AND TECHNICAL INFORMATION OFFICE

NATIONAL AERONAUTICS AND SPACE ADMINISTRATION

Washington, D.C. 20546